

May 2001

**Solutions of the atmospheric, solar and LSND neutrino anomalies
from TeV scale quark-lepton unification**

T. L. Yoon and R. Foot

*School of Physics
Research Centre for High Energy Physics
The University of Melbourne
Victoria 3010 Australia*

Abstract

There is a unique $SU(4) \otimes SU(2)_L \otimes SU(2)_R$ gauge model which allows quarks and leptons to be unified at the TeV scale. It is already known that the neutrino masses arise radiatively in the model and are naturally light. We study the atmospheric, solar and LSND neutrino anomalies within the framework of this model.

arXiv:hep-ph/0105101v2 20 Aug 2001

I. INTRODUCTION

The similarity of the quarks and leptons may be due to some type of symmetry between them. Various theories have been proposed including the Pati-Salam theory [1] where the leptons take the fourth colour within a $SU(4) \otimes SU(2)_L \otimes SU(2)_R$ gauge model*. While definitely a good idea, there are some slightly unpleasant aspects of the Pati-Salam model. In particular, one of the main drawbacks of the Pati-Salam theory is that almost all of its unique predictions for new physics cannot be tested because the experimental constraints on the symmetry breaking scale imply that it is out of reach of current and proposed experiments. The problem is twofold. First there are stringent constraints coming from rare meson decays. These imply a lower limit on the symmetry breaking scale of about 20 TeV [3] for the symmetry breaking scale which means that the heavy gauge bosons are too heavy to be found in even the Large Hadron Collider (LHC). The Pati-Salam model at the relatively low scale of 20 TeV also has great problems in explaining the light neutrino masses. The see-saw mechanism adopted in such models cannot suppress the neutrino mass sufficiently unless the symmetry breaking scale is very high. The required light neutrino masses suggest that the symmetry breaking scale is at least about 50 PeV [4] (1 PeV \equiv 1000 TeV). All is not lost however. There appears to be a unique alternative $SU(4) \otimes SU(2)_L \otimes SU(2)_R$ gauge model (which we call the alternative 422 model) which preserves the elegance and simplicity of the original Pati-Salam theory while allowing for a low symmetry breaking scale of about 1 TeV [5]. This not only allows the unique predictions of the theory to be tested in collider experiments, but the theory also avoids the dreaded gauge hierarchy problem by not introducing any hierarchy to begin with. The theory also has characteristic predictions for rare B, K decays, baryon number violation as well as non-zero neutrino masses, all of which are naturally within current bounds, despite the low symmetry breaking scale of a TeV. Thus in one act of prestidigitation all of the problems afflicting the original Pati-Salam model are cured.

Over the last few years, significant evidence for neutrino masses has emerged from the neutrino physics anomalies: the atmospheric [6], solar [7] and LSND [8] neutrino experiments. It is therefore an interesting question as to whether the alternative 422 model can accommodate these experiments. It has already been shown [9] that the masses for the neutrinos in this model typically span the necessary range to possibly account for these experiments. In fact viewed simply as a gauge model for neutrino masses, the theory is quite interesting because it provides a nice explanation for the small masses of the neutrinos without any need for (untestable) hypothesis about high energy scales (which arise in most popular theories of neutrino masses). We will show that the theory in its minimal form can accommodate the atmospheric and LSND neutrino anomalies but not all three (including solar) simultaneously. Thus, the theory is a candidate for the physics responsible for the neutrino physics anomalies. However, since it cannot explain all three of the neutrino anomalies, it obviously follows that if all three anomalies are confirmed in forthcoming

* Other possibilities include models with a discrete quark-lepton symmetry which features a spontaneously broken $SU(3)$ colour group for leptons. [2]

experiments, then this would require physics beyond this model for an explanation. One elegant possibility is the mirror symmetrized extension which can provide a simple explanation of the neutrino physics anomalies, as we will show.

The outline of this paper is as follows: In section II we briefly comment on the experimental situation and the various oscillation solutions to the solar, atmospheric neutrino anomalies and the LSND measurements. In section III we revise the essentials of the alternative 422 model. In particular we will derive the mass matrices of the fermions after spontaneous symmetry breaking (SSB). We will also define a basis for the fermions in which their weak eigenstates are related to their respective mass eigenstates via CKM-type unitary matrices. In section IV we explain the mechanisms that give rise to the masses of the neutrinos. This includes the tree level mixing that generates right-handed neutrino Majorana masses $^\dagger \tilde{\nu}_R M_R (\tilde{\nu}_R)^c$ and two radiative mechanisms, via gauge and scalar interactions, that give rise to Dirac masses of the ordinary neutrinos. In section V we consider the special case of decoupled generations and examine the possibility to obtain near maximal $\tilde{\nu}_L \rightarrow (\tilde{\nu}_R)^c$ oscillations within the model (which turns out to be negative). In section VI, we mirror symmetrise the alternative 422 model to obtain a TeV scale solution scheme for all three of the neutrino anomalies. In section VII we will identify how the minimal alternative 422 model could provide simultaneous solutions to (near maximal oscillations) atmospheric neutrino anomaly and the LSND measurements in the case where gauge interactions dominates the radiative neutrino mass generation. We conclude in section VIII.

II. OSCILLATION SOLUTIONS TO THE ATMOSPHERIC AND SOLAR NEUTRINO ANOMALIES AND LSND MEASUREMENTS

The experimental situation regarding the oscillation solutions of the atmospheric and solar neutrino problems has made much progress over the last few years. In this paper we mainly focus on the simplest possible solutions which involve maximal (or near maximal) two-flavour oscillations.

A. Atmospheric neutrino anomaly

In the case of atmospheric neutrino anomaly there is compelling evidence that about half of the up-going ν_μ flux disappears [6]. The simplest oscillation solutions which can explain the data are maximal $\nu_\mu \rightarrow \nu_\tau$ or maximal $\nu_\mu \rightarrow \nu_{sterile}$ oscillations [10]. Despite impressive efforts by Super-Kamiokande [11] the experimental data cannot yet distinguish between these two possibilities [12]. Unfortunately, this situation probably cannot be clarified until long-baseline experiments provide or fail to provide τ events approximately in the year 2007.

[†]Throughout this paper the tilde on the fermion fields is to signify that they are flavour eigenstates as opposed to mass eigenstates (without a tilde) in this model. See Section III for more detail. Note that the tilde has nothing to do with supersymmetry other than a mere notation coincidence.

At present the parameter range that is consistent with the atmospheric neutrino anomaly is roughly $\sin^2 2\theta \gtrsim 0.85$ and

$$10^{-3} \lesssim \delta m_{atm}^2 / \text{eV}^2 \lesssim 10^{-2}. \quad (1)$$

B. Solar neutrino anomaly

In the case of solar neutrino anomaly [7] there is very strong evidence that about half of the ν_e flux from the sun has gone missing when compared to theoretical models. The simplest explanation of this is in terms of maximal ν_e oscillations, with the main suspects being maximal $\nu_e \rightarrow \nu_\alpha$ (ν_α is some linear combination of ν_μ or ν_τ) [13–16] or maximal $\nu_e \rightarrow \nu_{sterile}$ oscillations [15–17][‡]. This maximum oscillation solution to the solar neutrino problem can explain the 50 % flux reduction for a large parameter range:

$$3 \times 10^{-10} \text{ eV}^2 \lesssim \delta m^2 \lesssim 10^{-3} \text{ eV}^2. \quad (2)$$

The upper bound arises from the lack of $\bar{\nu}_e$ disappearance in the CHOOZ and Palo Verde experiments [19], while the lower bound comes from a lack of any distortion in the measured Super-Kamiokande recoil energy spectrum [20,21], which should make its appearance for $\delta m^2 \lesssim 3 \times 10^{-10} \text{ eV}^2$ (traditional ‘just so’ region). Note that, the maximum oscillation solution was the only oscillation solution to predict the approximate energy independent spectrum obtained by Super-Kamiokande. (SMA MSW, LMA MSW and ‘Just So’ all predicted some distortion that should have been seen.) The Super-Kamiokande collaboration has also searched for a day-night effect. However no evidence for any difference in the day and night time event rates were found with a 3σ upper limit of [20]

$$A_{n-d} < 0.055 \quad (3)$$

where $A_{n-d} \equiv (N - D)/(N + D)$ ($N =$ night time events and $D =$ day time events). This limit allows a slice of parameter space to be excluded (using the numerical results of Ref. [17]):

$$\begin{aligned} 2 \times 10^{-7} \text{ eV}^2 &\lesssim |\delta m_{solar}^2| \lesssim 10^{-5} \text{ eV}^2 && \text{(sterile)} \\ 4 \times 10^{-7} \text{ eV}^2 &\lesssim |\delta m_{solar}^2| \lesssim 2 \times 10^{-5} \text{ eV}^2 && \text{(active)}. \end{aligned} \quad (4)$$

Thus for both the active and sterile maximal oscillation solutions the allowed δm^2 range breaks up into a high δm^2 region and a low δm^2 region:

$$\begin{aligned} 2y \times 10^{-5} &\lesssim \delta m^2 / \text{eV}^2 \lesssim 10^{-3} && \text{(high } \delta m^2 \text{ region)} \\ 3 \times 10^{-10} &\lesssim \delta m^2 / \text{eV}^2 \lesssim 4y \times 10^{-7} && \text{(low } \delta m^2 \text{ region)}, \end{aligned} \quad (5)$$

[‡]Note that maximal (or near maximal) $\nu_e \rightarrow \nu_{sterile}$ oscillations (and/or maximal $\nu_\mu \rightarrow \nu_{sterile}$ oscillations) are consistent with standard big-bang nucleosynthesis (BBN) for a large range of parameters [18].

where $y = 0.5$ for sterile case and $y = 1$ for the active case. These oscillation solutions will be tested in the near future by SNO, Borexino and KamLAND experiments. In fact the SNO experiment has recently announced their first results [22] which is a measurement of the charged current event rate. This result, when combined with the elastic scattering rate obtained at super-Kamiokande disfavors the $\nu_e \rightarrow \nu_{sterile}$ oscillation solution at about the 3 sigma level [22]. However both measurements are dominated by systematics which suggests that this result is not yet convincing but is nevertheless an interesting hint. Things should become much clearer when SNO measures the neutral current event rate which should allow $\nu_e \rightarrow \nu_\alpha$ to be distinguished from $\nu_e \rightarrow \nu_{sterile}$ at more than 7 sigma. Meanwhile, Borexino [23] can test the low δm^2 region by searching for a day-night effect and also seasonal effects [16] while KamLAND [24] can test the high δm^2 region by searching for ν_e disappearance. Finally part of the high δm^2 region, $10^{-4} \lesssim \delta m^2/\text{eV}^2 \lesssim 10^{-3}$ impacts on the atmospheric electron-like events and is currently disfavoured [25].

C. LSND data

There is strong and interesting evidence for $\bar{\nu}_\mu \rightarrow \bar{\nu}_e$ oscillations coming from the LSND experiment [8] which suggests the parameter region

$$0.2 \lesssim \delta m_{LSND}^2/\text{eV}^2 \lesssim 3 \quad (6)$$

with a rather small mixing angles $\sin^2 2\theta \sim 3 \times 10^{-2} - 10^{-3}$. This result will be checked by BooNE [26] soon. If the LSND signal is verified then one must invoke additional (sterile) neutrino(s) to simultaneously explain all the solar, atmospheric and LSND data due to the large $\delta m_{LSND}^2 \sim \text{eV}^2$ gap. Even if LSND is not verified, effectively sterile neutrino may still be responsible for the solar and/or atmospheric neutrino anomalies. The origin of the atmospheric and solar neutrino anomalies is something that only careful experimental studies can establish.

III. THE MODEL

In this paper we shall study the physics of the neutrino masses in the alternative 422 model [5,9]. Before doing so it is instructive to revise the essentials of this model (with some refinement). The gauge symmetry of the alternative 422 model is

$$SU(4) \otimes SU(2)_L \otimes SU(2)_R. \quad (7)$$

Under this gauge symmetry the fermions of each generation transform in the anomaly free representations:

$$Q_L \sim (4, 2, 1), \quad Q_R \sim (4, 1, 2), \quad f_L \sim (1, 2, 2). \quad (8)$$

The minimal choice of scalar multiplets which can both break the gauge symmetry correctly and give all of the charged fermions mass is

$$\chi_L \sim (4, 2, 1), \quad \chi_R \sim (4, 1, 2), \quad \phi \sim (1, 2, 2). \quad (9)$$

Observe that the required scalar multiplets have the same gauge representation as those of the fermions which gives some degree of elegance to the scalar sector (although there are three generations of fermions and only one generation of scalars). These scalars couple to the fermions as follows:

$$\mathcal{L} = \lambda_1 \text{Tr} \left[\overline{Q}_L (f_L)^c \tau_2 \chi_R \right] + \lambda_2 \text{Tr} \left[\overline{Q}_R f_L^T \tau_2 \chi_L \right] + \lambda_3 \text{Tr} \left[\overline{Q}_L \phi \tau_2 Q_R \right] + \lambda_4 \text{Tr} \left[\overline{Q}_L \phi^c \tau_2 Q_R \right] + \text{H.c.}, \quad (10)$$

where the generation index has been suppressed and $\phi^c = \tau_2 \phi^* \tau_2$. Under the $SU(3)_c \otimes U(1)_T$ subgroup of $SU(4)$, the 4 representation has the branching rule $4 = 3(1/3) + 1(-1)$. We will assume that the $T = -1, I_{3R} = 1/2$ ($I_{3L} = 1/2$) components of χ_R (χ_L) gain non-zero Vacuum Expectation Values (VEVs) as well as the $I_{3L} = -I_{3R} = -1/2$ and $I_{3L} = -I_{3R} = 1/2$ components of the ϕ . We denote these VEVs by $w_{R,L}, u_{1,2}$ respectively. In other words,

$$\begin{aligned} \langle \chi_R(T = -1, I_{3R} = 1/2) \rangle &= w_R, & \langle \chi_L(T = -1, I_{3L} = 1/2) \rangle &= w_L, \\ \langle \phi(I_{3L} = -I_{3R} = -1/2) \rangle &= u_1, & \langle \phi(I_{3L} = -I_{3R} = 1/2) \rangle &= u_2. \end{aligned} \quad (11)$$

We will assume that the VEVs satisfy $w_R > u_{1,2}, w_L$ so that the symmetry is broken as follows:

$$\begin{aligned} &SU(4) \otimes SU(2)_L \otimes SU(2)_R \\ &\quad \downarrow \langle \chi_R \rangle \\ &SU(3)_c \otimes SU(2)_L \otimes U(1)_Y \\ &\quad \downarrow \langle \phi \rangle, \langle \chi_L \rangle \\ &SU(3)_c \otimes U(1)_Q \end{aligned} \quad (12)$$

where $Y = T + 2I_{3R}$ is the linear combination of T and I_{3R} which annihilates $\langle \chi_R \rangle$ (i.e. $Y \langle \chi_R \rangle = 0$) and $Q = I_{3L} + \frac{Y}{2}$ is the generator of the unbroken electromagnetic gauge symmetry. Observe that in the limit where $w_R \gg w_L, u_1, u_2$, the model reduces to the standard model. The VEV w_R breaks the gauge symmetry to the standard model subgroup.

To facilitate easy reference, we will use $\alpha = \pm \frac{1}{2}, \beta = \pm \frac{1}{2}$ to index the $SU(2)_L$ and $SU(2)_R$ component respectively, whereas $\gamma \equiv \{\gamma', 4\}$ is used to index the $SU(4)$ components, where $\gamma' \equiv (y, g, b)$ is the usual colour index for $SU(3)_c$, and $\gamma = 4$ the forth colour. With this index scheme the fermion multiplets are written as (with the generation index suppressed)

$$Q_L^{\alpha, \gamma} = \begin{pmatrix} \tilde{U} & \tilde{E}^0 \\ D & \tilde{E}^- \end{pmatrix}_L, \quad Q_R^{\beta, \gamma} = \begin{pmatrix} \tilde{U} & \tilde{\nu} \\ \tilde{D} & l \end{pmatrix}_R, \quad f_L^{\alpha, \beta} = \begin{pmatrix} (\tilde{E}_R^-)^c & \tilde{\nu}_L \\ (\tilde{E}_R^0)^c & l_L \end{pmatrix}. \quad (13)$$

The rationale to label some of the fermion fields in the multiplets with a tilde will be addressed shortly in the next paragraph. In the above matrices the first row of Q_L and f_L (Q_R) is the I_{3L} (I_{3R}) = α (β) = $1/2$ component while the second row is the I_{3L} (I_{3R}) = α (β) = $-1/2$ component. The two columns of Q_L, Q_R are the $\gamma = \gamma'$ and $\gamma = 4$ components

of $SU(4)$, and the columns of f_L are the $I_{3R} = \beta = \pm 1/2$ components. Each field in the multiplets Eq. (13) represents 3×1 column vector of three generations.

As in the case of the Standard Model, the flavour states of the fermion fields are, in general, not aligned with the corresponding mass eigenstates. This shall necessitate the introduction of some theoretically arbitrary CKM-type unitary matrices into the theory. Without loss of generality we can choose a basis such that D_L (the left-handed down-type quarks) in Q_L , l_R (the right-handed charged leptons fields) in Q_R and l_L (left-handed charged lepton fields) in f_L are (almost [§]) mass eigenstate fields that couple with their respective diagonal mass matrix. The rest of the fields $\tilde{\psi}$ (fields with a tilde) are flavour states.

It is instructive to list and label the scalar fields index explicitly as follows:

$$\chi_L^{\alpha,\gamma} = \begin{pmatrix} \chi_L^{\gamma',\frac{1}{2}} & \chi_L^{4,\frac{1}{2}} \\ \chi_L^{\gamma',-\frac{1}{2}} & \chi_L^{4,-\frac{1}{2}} \end{pmatrix}, \quad \chi_R^{\beta,\gamma} = \begin{pmatrix} \chi_R^{\gamma',\frac{1}{2}} & \chi_R^{4,\frac{1}{2}} \\ \chi_R^{\gamma',-\frac{1}{2}} & \chi_R^{4,-\frac{1}{2}} \end{pmatrix}, \quad \phi^{\alpha,\beta} = \begin{pmatrix} \phi^{\frac{1}{2},\frac{1}{2}} & \phi^{\frac{1}{2},-\frac{1}{2}} \\ \phi^{-\frac{1}{2},\frac{1}{2}} & \phi^{-\frac{1}{2},-\frac{1}{2}} \end{pmatrix}. \quad (14)$$

The electric charges of the components of $\chi_{L,R}$, ϕ can be read off from Eq. (13) because the scalars and fermions have the same gauge representation.

The mass matrices (after spontaneous symmetry breaking) of the fermions are derived from the Yukawa Lagrangian of Eq. (10) as follows:

$$\mathcal{L} \text{ (after SSB)} = \mathcal{L}^E + \mathcal{L}^l + \mathcal{L}^u + \mathcal{L}^d + \text{H.c.}, \quad (15)$$

where

$$\begin{aligned} -i\mathcal{L}^E &= \overline{\tilde{E}_L} \tilde{M}_E \tilde{E}_R^- - \overline{\tilde{E}_L^0} \tilde{M}_E \tilde{E}_R^0, & -i\mathcal{L}^l &= \overline{(\tilde{E}_R^0)^c} M_l \tilde{\nu}_R + \bar{l}_L M_l l_R, \\ -i\mathcal{L}^u &= \overline{\tilde{U}_L} \tilde{M}_u \tilde{U}_R + \overline{\tilde{E}_L^0} \tilde{M}_u \tilde{\nu}_R, & -i\mathcal{L}^d &= -\overline{\tilde{D}_L} \tilde{M}_d \tilde{D}_R - \overline{\tilde{E}_L^-} \tilde{M}_d l_R, \end{aligned} \quad (16)$$

and

$$\tilde{M}_E = w_R \lambda_1, \quad \tilde{M}_u = (\lambda_3 u_2 - \lambda_4 u_1), \quad \tilde{M}_d = (\lambda_4 u_2 - \lambda_3 u_1), \quad (17)$$

are 3×3 generally non-diagonal mass matrices for the exotic E leptons, up-type quarks U and down-type quarks D respectively.

$$M_l = w_L \lambda_2 = \begin{pmatrix} m_e & 0 & 0 \\ 0 & m_\mu & 0 \\ 0 & 0 & m_\tau \end{pmatrix} \quad (18)$$

is the diagonal mass matrix for the charged leptons. The mass matrices \tilde{M}_E , \tilde{M}_u , \tilde{M}_d can be diagonalised in the usual way (biunitary diagonalisation) to obtain the diagonal mass matrices, e.g. $M_E = U^\dagger \tilde{M}_E V$ etc. so that the flavour states $\tilde{\psi}$ are related to their mass eigenstates ψ via unitary matrices:

[§] Strictly, l_L, l_R are approximately but not exactly mass eigenstates because of the mass mixing between l_R and \tilde{E}_L^- [see the forthcoming Eq. (16)]. This means that the true charged lepton mass eigenstate fields have the form $l_L^{true} = l_L + \mathcal{O}(\frac{M_d M_l}{M_E^2}) E_L$, $l_R^{true} = l_R + \mathcal{O}(\frac{M_d}{M_E}) E_R$.

$$\begin{aligned}
E_R &= V^\dagger \tilde{E}_R, & E_L &= U^\dagger \tilde{E}_L, \\
U_R &= Y_R^\dagger \tilde{U}_R, & U_L &= Y_L^\dagger \tilde{U}_L, \\
D_R &= K' \tilde{D}_R,
\end{aligned}
\tag{19}$$

and $\tilde{D}_L = D_L, \tilde{l}_L = l_L, \tilde{l}_R = l_R$ with our choice of basis. Note that approximately the same unitary matrix U (V) relates both E_L^0, E_L^- (E_R^0, E_R^-) to their weak eigenstates $\tilde{E}_L^0, \tilde{E}_L^-$ ($\tilde{E}_R^0, \tilde{E}_R^-$) because the mass matrices are approximately $SU(2)_L$ ($SU(2)_R$) invariant.

The gauge fields in the 15 representation of $SU(4)$ has the branching rule $15 = 8(0) + 3(-\frac{4}{3}) + \bar{3}(\frac{4}{3}) + 1(0)$ under $SU(3)_L \otimes U(1)_T$. We identify the colour octet $8(0)$ as the gluons of the usual $SU(3)_c$ colour group, $3(-\frac{4}{3}), \bar{3}(\frac{4}{3})$ colour triplet lepto-quark gauge bosons W', W'^* that couple the $\gamma = \gamma'$ components to $\gamma = 4$ component in $\chi_{L,R}, Q_{L,R}$. Note that there is also a neutral gauge boson B'_μ corresponds to the singlet $1(0)$. The matrix $Y_L^\dagger \equiv K_L$ is the usual CKM matrix (as in the Standard Model), whereas $Y_R^\dagger K'^\dagger \equiv K_R$ is the analogue of the CKM matrix for the right-handed charged quarks in $SU(2)_R$ sector. The matrix K' is the analogue of the CKM-type matrix in the $SU(4)$ sector pertaining to lepto-quark interactions mediated by W', W'^* . It was shown in Ref. [5,9] that the main experimental constraints on this 422 model come from rare B and K decays such as $K^0 \rightarrow \mu^\pm e^\mp, B^0 \rightarrow \mu^\pm \tau^\mp$ etc. depending on the form of K' . Remarkably, the symmetry breaking scale could be as low as a TeV without being in conflict with any experimental measurements. Indeed we will assume that the symmetry breaking scale is in the interesting low range:

$$0.5(1.0) \text{ TeV} \lesssim M_{W_R}(M_{W'}) \lesssim 10 \text{ TeV}, 45 \text{ GeV} \lesssim M_E \lesssim 10 \text{ TeV}, \tag{20}$$

which is well motivated because it avoids the gauge hierarchy problem and it also allows the model to be testable at existing and future colliders (such as LHC). (Note that the lower limit on the mass of the E lepton arises from LEP measurements of the Z^0 width).

Apart from laboratory experimental bounds, there are also astrophysical ones on M_{W_R} . In particular Ref. [27–29] have argued that based on ‘energy-loss’ argument, Supernova 1987A excludes a range of values for M_{W_R} and the $W_L - W_R$ mixing parameter, ζ ** (for $m_{\nu_R} \lesssim 10 \text{ MeV}$):

$$\begin{aligned}
\zeta &< 10^{-5}, \\
(0.3 - 0.5) &\lesssim \frac{M_{W_R}}{\text{TeV}} \lesssim 22 - 40 \quad \text{in the limit } \zeta \rightarrow 0,
\end{aligned}
\tag{21}$$

which seems to marginally rule out the range of M_{W_R} as assumed in Eq. (20). However, while there will undoubtedly be effects for supernova coming from the additional gauge bosons in our model, we should nonetheless keep in mind that the modeling of core collapse of supernova is generally plagued by theoretical, observational as well numerical uncertainties. For example, Berezhinsky [30] has recently emphasised that the reasonably successful

**In our case here, $\zeta \simeq \frac{\mu^2}{M_{W_R}^2} \lesssim 4 \times 10^{-5} - 1 \times 10^{-4}$, where $\mu^2 = g_L g_R u_1 u_2$, see forth coming Eq. (33).

description of SN1987A is somewhat surprising given that it was assumed that the presupernova protostar was a non-rotating red super giant, while it appears that it was actually a rotating blue super giant. Also, Turner [31] pointed out that there exists uncertainty in the theoretical model for the hot core of a core collapsed supernova, which itself depends critically upon the equation of state at supernuclear densities (which is a state-of-art problem in nuclear physics). The criterion of neutrino luminosity from SN 1987A, $Q_a \lesssim 10^{53}$ erg s⁻¹, a key ingredient in obtaining the SN 1987A bound of Eq. (21), according to Ref. [31] is also subjected to question. Raffelt and Seckel [27] pointed out that SN 1987A bound on the right-handed and other light exotic particle interactions could be uncertain up to as much as 2 order of magnitude, in which case could render the apparent ‘conflict’ of the range assumed by Eq. (20) and the SN 1987A bound of Eq. (21) be alleviated. While keeping in mind the possible astrophysical implications of a low symmetry breaking scale $M_{W_R} \sim 1$ TeV, we now continue with our exploration of the possible phenomenology of the alternative 422 model.

The $SU(2)_{L,R}$ charged gauge bosons $W_{L,R}^\pm$ couple to the fermions via the interaction Lagrangian density

$$\begin{aligned}
i\mathcal{L}^{gauge} = & \frac{g_L}{\sqrt{2}} [\overline{U}_L W_L^+ K_L D_L + \overline{\nu}_L W_L^+ l_L + \overline{E}_L^0 W_L^+ E_L^- + \overline{(E_R^-)^c} W_L^+ (E_R^0)^c + \text{H.c.}] \\
& + \frac{g_R}{\sqrt{2}} [\overline{U}_R W_R^+ K_R D_R + \overline{\nu}_R W_R^+ l_R + \overline{(E_R^0)^c} V^\dagger W_R^+ l_L + \overline{(E_R^-)^c} V^\dagger W_R^+ \tilde{\nu}_L \\
& + \text{H.c.}].
\end{aligned} \tag{22}$$

The charged gauge interactions are of our interest because they will give rise to radiative Dirac mass terms to the neutrinos in this model as we will now discuss.

IV. NEUTRINO MASS

With the model as defined in Section III, the ordinary neutrinos $\tilde{\nu}_L$ are massless at tree level because the $\tilde{\nu}_L$ states do not couple to any VEV [see Eq. (15)]^{††}. However, the neutrino masses are non-zero in the model because there are 1-loop (and higher order) Feynman diagrams which contribute to their masses. In other words the masses of the neutrinos arise radiatively in the model. In particular, as we will see later, a Dirac mass m_D and a $\tilde{\nu}_L - (E_L)^c$ mass mixing term $m_{\nu E}$ will be generated as mass corrections at 1-loop level, meanwhile the $\tilde{\nu}_R$ states gain Majorana masses at tree-level by mixing with E leptons. We

^{††}To generate tree-level neutrino mass we need to either admit the gauge invariant bare mass term $m_{bare} \overline{f}_L (f_L)^c$ into the Lagrangian density in Eq. (10) or add a new Higg $\Delta \sim (4, 2, 3)$ into the Lagrangian density via the coupling $\lambda_\Delta \Delta^\dagger \overline{Q}_R f_L + \text{H.c.}$. By developing a VEV, Δ can generate a Dirac mass term $\overline{\nu}_L m_D \tilde{\nu}_R$. We argue that, since the scale of m_{bare} is completely independent of the weak scale, the assumption that $m_{bare} \ll M_{weak}$ is surely an interesting possibility. In view of this plausible assumption we have set $m_{bare} = 0$. Meanwhile, adding an additional scalar multiplet such as Δ spoils both the simplicity and elegance of the model.

will elaborate these mechanisms in more detail in the following subsections. In this paper we will be working exclusively in the t'Hooft-Feynman gauge.

A. Tree level Majorana mass matrix M_R

At tree level, mixing between $\tilde{\nu}_R$ with $E_{L,R}^0$ generates right-handed neutrino Majorana mass M_R . In the mass eigenstate basis (for the $E_{L,R}^0$) defined in Eq. (19), the tree-level Lagrangian density of Eq. (15) becomes

$$\begin{aligned}
-i\mathcal{L} = & \frac{1}{2} \left(\overline{\tilde{\nu}_L} \quad \overline{(\tilde{\nu}_R)^c} \quad \overline{E_L^0} \quad \overline{(E_R^0)^c} \right) \mathbf{M} \begin{pmatrix} (\tilde{\nu}_L)^c \\ \tilde{\nu}_R \\ (E_L^0)^c \\ (E_R^0) \end{pmatrix} \\
& - \left(\overline{D_L} \quad \overline{E_L^-} \right) \begin{pmatrix} M_d & 0 \\ 0 & U^\dagger M_d K' \end{pmatrix} \begin{pmatrix} D_R \\ l_R \end{pmatrix} \\
& + \overline{E_L^-} M_E E_R^- + \overline{l_L} M_l l_R + \overline{U_L} M_u U_R + \text{H.c.}, \tag{23}
\end{aligned}$$

where

$$\mathbf{M} = \begin{pmatrix} 0 & 0 & 0 & 0 \\ 0 & 0 & Y_R M_u Y_L^\dagger U & M_l V \\ 0 & (Y_R M_u Y_L^\dagger U)^\dagger & 0 & -M_E \\ 0 & (M_l V)^\dagger & -M_E & 0 \end{pmatrix} \quad (12 \times 12 \text{ matrix}). \tag{24}$$

M_d , M_u are the 3×3 diagonal mass matrices for the down-type quarks and up-type quarks respectively, whereas M_E is the 3×3 diagonal mass matrix for E leptons after biunitary-diagonalising $\tilde{M}_E = w_L \lambda_1$:

$$\tilde{M}_E = U M_E V^\dagger \equiv U \begin{pmatrix} M_{E_1} & 0 & 0 \\ 0 & M_{E_2} & 0 \\ 0 & 0 & M_{E_3} \end{pmatrix} V^\dagger. \tag{25}$$

The matrices U, V describe the relation between the weak and mass eigenstates of the E leptons and can be determined from λ_1 [see Eq. (19)].

One can block diagonalise the 9×9 matrix in the lower right sector of \mathbf{M} by a similarity transformation [32] using the approximately orthogonal matrix

$$U_\rho = \begin{pmatrix} \mathbf{I}_3 & \rho_p \\ -\rho_p^T & \mathbf{I}_6 \end{pmatrix} \quad (9 \times 9 \text{ matrix})$$

where

$$\rho_p = \begin{pmatrix} Y_R M_u Y_L^\dagger U & M_l V \end{pmatrix} \begin{pmatrix} 0 & -M_E^{-1} \\ -M_E^{-1} & 0 \end{pmatrix}. \quad (3 \times 6 \text{ matrix}) \tag{26}$$

Block diagonalisation casts \mathbf{M} into the form

$$\mathbf{M} \rightarrow \begin{pmatrix} 0 & 0 & 0 & 0 \\ 0 & M_R & 0 & 0 \\ 0 & 0 & -\mathbf{M}'_E \\ 0 & 0 & -\mathbf{M}'_E \end{pmatrix}, \quad (27)$$

where each '0' is a 3×3 matrix of zeros, and

$$\begin{aligned} M_R &\simeq \left(M_l V M_E^{-1} U^\dagger Y_L M_u Y_R^\dagger \right) + \left(M_l V M_E^{-1} U^\dagger Y_L M_u Y_R^\dagger \right)^\dagger, \quad (3 \times 3 \text{ matrix}) \\ \mathbf{M}'_E &\simeq \begin{pmatrix} 0 & M_E \\ M_E & 0 \end{pmatrix}. \quad (6 \times 6 \text{ matrix}) \end{aligned} \quad (28)$$

In the limit $M_E \gg M_l, M_u$, the states $\tilde{\nu}_R$ are decoupled from the E leptons. In the special case of decoupled generations (e.g. $Y_L = Y_R = U = V = \mathbf{I}$), \mathbf{M} reduces to

$$\mathbf{M} = \begin{pmatrix} 0 & 0 & 0 & 0 \\ 0 & 0 & m_{q_u} & m_l \\ 0 & m_{q_u} & 0 & -M_{E_i} \\ 0 & m_l & -M_{E_i} & 0 \end{pmatrix}, \quad (29)$$

where i, q_u and l index the generations. In this case, Eq. (28) reproduces the result

$$M_R = \frac{2m_{q_u} m_l}{M_{E_i}} \quad (30)$$

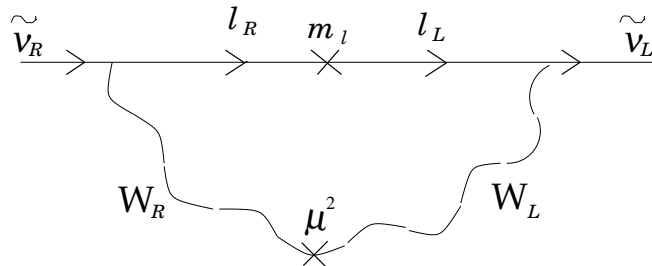
as obtained in Ref. [9].

B. Radiative correction to \mathbf{M} due to gauge interactions

At the 1-loop level the gauge interactions from the charged $SU(2)_L$ gauge bosons W_L^\pm and $SU(2)_R$ gauge bosons W_R^\pm give rise to $\tilde{\nu}_L(\tilde{\nu}_L)^c$ Majorana mass m_M , $\tilde{\nu}_L\tilde{\nu}_R$ Dirac mass m_D and $\tilde{\nu}_L(E_L^0)^c$ mass mixing term $m_{\nu E}$. The Dirac mass m_D arises from the gauge interactions^{‡‡}

$$\frac{g_L}{\sqrt{2}} \tilde{\nu}_L W_{\mu L}^+ l_L + \frac{g_R}{\sqrt{2}} \tilde{\nu}_R W_{\mu R}^+ l_R + \text{H.c.} \quad (31)$$

which leads to the Feynman diagram:



^{‡‡}The (unphysical) Goldstone boson contributions will be evaluated together with the (physical) scalar contributions in Part C of this section.

Figure 1. Dirac mass generated by gauge interactions leading to the mass term $\overline{\tilde{\nu}_L}\tilde{\nu}_R$.

Note that since these interactions do not mediate cross generational mixing among the neutrinos, the Dirac mass matrix m_D is strictly diagonal. As calculated in Ref. [9], for each generation,

$$m_D = m_l \frac{g_R g_L}{8\pi^2} \frac{\mu^2}{M_{W_R}^2} \ln \left(\frac{M_{W_R}^2}{M_{W_L}^2} \right) \equiv m_l k_g, \quad (32)$$

where $\mu^2 \equiv g_L g_R u_1 u_2$ is the $W_L - W_R$ mixing mass. Note, that the lower limit of μ^2 is simply zero since μ^2 vanishes in either limits of $u_1 \rightarrow 0$ or $u_2 \rightarrow 0$ and the theory remains phenomenologically consistent in this limit. It was also shown in the Ref. [9] that

$$\frac{\mu^2}{M_{W_R}^2} \lesssim \frac{1}{2\sqrt{3}} \frac{M_{W_L}^2}{M_{W_R}^2} \frac{m_b}{m_t}, \quad (33)$$

which is not a strict upper limit, but rather an approximate condition to avoid fine tuning^{§§}. In view of this rough upper limit, it is convenient to write m_D in terms of a parameter $0 < \eta < 1$ defined such that

$$m_D = m_l k_g = m_l \eta S \quad (34)$$

where

$$\begin{aligned} S &= S(M_{W_R}) = \frac{g_R g_L}{8\pi^2} \ln \left(\frac{M_{W_R}^2}{M_{W_L}^2} \right) \frac{1}{2\sqrt{3}} \frac{M_{W_L}^2}{M_{W_R}^2} \frac{m_b}{m_t} \\ &\sim 10^{-7} \left(\frac{\text{TeV}}{M_{W_R}} \right)^2. \end{aligned} \quad (35)$$

If we take the reasonable range of $0.5 \text{ TeV} < M_{W_R} \lesssim 10 \text{ TeV}$, then S typically spans a range of

$$10^{-6} < S \lesssim 10^{-9}. \quad (36)$$

Thus, the gauge loop contribution to m_D is proportional to m_l and is naturally light because of its radiative origin.

The mass mixing term $m_{\nu E}$ arises at 1-loop level via the gauge interactions

$$\frac{g_L}{\sqrt{2}} \overline{E_L^0} W_{\mu L}^+ E_L^- + \frac{g_R}{\sqrt{2}} \overline{(E_R^-)^c} V^\dagger W_{\mu R}^+ \tilde{\nu}_L + \text{H.c.} \quad (37)$$

leading to the Feynman diagram:

^{§§}As shown in Ref. [9], the limit of Eq. (33) comes from $\frac{u_1 u_2}{u_1^2 + u_2^2} \lesssim \frac{m_b}{m_t}$. To avoid the equality $m_b = m_t$ we will need the scale of u_1, u_2 be separated by a hierarchy, else we will need to fine-tune the Yukawa coupling constants $\lambda_{3,4}$.

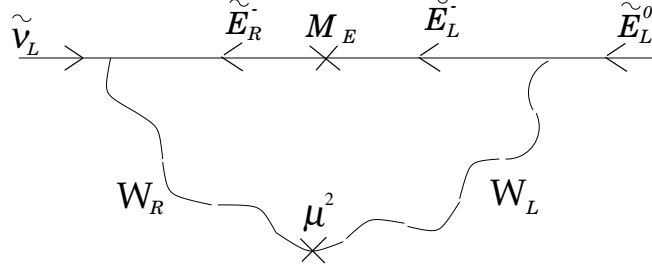


Figure 2. $\overline{\tilde{\nu}_L}(\tilde{E}_L^0)^c$ neutrino mixing term generated by gauge interactions leading to the mass term $m_{\nu E}$.

Note that in contrast to m_D , the involvement of the matrix V in the interactions Eq. (37) may mediate cross generational mixing. In the special case of decoupled generations, $m_{\nu E}$ has been calculated earlier by Ref. [9] as

$$m_{\nu E} = M_E \frac{g_R g_L}{8\pi^2} \left(\frac{\mu^2}{M_{W_R}^2} \right) \left[\ln \left(\frac{M_{W_R}^2}{M_{W_L}^2} \right) + \frac{M_E^2 \ln \left(\frac{M_{W_L}^2}{M_E^2} \right)}{M_E^2 - M_{W_L}^2} - \frac{M_E^2 \ln \left(\frac{M_{W_R}^2}{M_E^2} \right)}{M_E^2 - M_{W_R}^2} \right] \sim \eta M_E S. \quad (38)$$

In addition to m_D and $m_{\nu E}$, this model also generates a $\overline{\tilde{\nu}_L}(\tilde{\nu}_L)^c$ Majorana mass term m_M at 1-loop level by charged gauge interactions. In the case of decoupled generations,

$$m_M = m_l m_{qd} M_E \frac{g_R g_L}{8\pi^2} \left(\frac{\mu^2}{M_{W_R}^2} \right) \left[\frac{\ln \left(\frac{M_{W_R}^2}{M_E^2} \right)}{M_{W_R}^2 - M_E^2} - \frac{\ln \left(\frac{M_{W_L}^2}{M_E^2} \right)}{M_{W_L}^2 - M_E^2} \right] \sim \eta \frac{m_l m_{qd}}{M_E} S \quad (39)$$

is generically tiny compared to m_D and $m_{\nu E}$.

C. Radiative correction to M due to scalar interactions

In the previous subsection we have shown that at 1-loop level the gauge interactions give rise to Dirac mass m_D , mass mixing correction $m_{\nu E}$ and also m_M . Nevertheless, in this model this is not the only way mass corrections could arise. Other than the gauge mechanism discussed in the previous subsection, the Higgs sector also contains interactions that could generate Dirac mass for the neutrinos as a radiative mass correction. The relevant interactions involve the negatively charged colour singlet scalar $\chi_{L,R}^{4,-\frac{1}{2}}$:

$$\begin{aligned} -i\mathcal{L}_{\chi^{4,-\frac{1}{2}}} &= -i\mathcal{L}_{\chi_L^{4,-\frac{1}{2}}} - i\mathcal{L}_{\chi_R^{4,-\frac{1}{2}}} \\ &= \frac{\chi_R^{4,-\frac{1}{2}}}{w_R} \overline{E_L^-} M_E V^\dagger (\tilde{\nu}_L)^c - \frac{\chi_L^{4,-\frac{1}{2}}}{w_L} \overline{\tilde{\nu}_R} M_l V (E_R^-)^c \\ &\quad - \frac{\chi_R^{4,-\frac{1}{2}}}{w_R} \overline{E_L^0} M_E V^\dagger (l_L)^c - \frac{\chi_L^{4,-\frac{1}{2}}}{w_L} \overline{l_R} M_l \tilde{\nu}_L + \text{H. c.} \end{aligned} \quad (40)$$

The first two terms of Eq. (40) will give rise to a Dirac mass correction m_D with E^- as propagator (see Fig. 3), whereas the last two terms will give rise to a mass mixing term $m_{\nu E}$ with charged leptons as propagator. Therefore in comparison to m_D the mass $m_{\nu E}$ can be safely ignored.

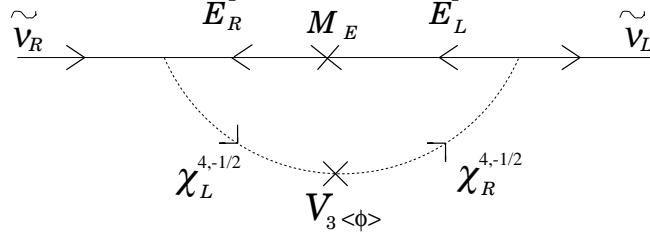


Figure 3. $\overline{\tilde{\nu}_L}\tilde{\nu}_R$ Dirac mass generated by scalar interactions. The cross in the scalar propagator is the perturbative mass mixing term that can be shown to vanish in either limit of $u_{1,2} \rightarrow 0$

The mixing between $\chi_L - \chi_R$ is effected solely by the mixing term of the form

$$\begin{aligned}
 V_3 &= M\chi_L^\dagger\phi\tau_2\chi_R + M'\chi_L^\dagger\phi^c\tau_2\chi_R + \text{H.c.} \\
 \Rightarrow V_{3\langle\phi\rangle} &= m_{3\langle\phi\rangle}^2\chi_L^{4,-\frac{1}{2}}\chi_R^{4,-\frac{1}{2}*} + \text{H.c.}; \\
 m_{3\langle\phi\rangle}^2 &\equiv -(Mu_1 + M'u_2)
 \end{aligned} \tag{41}$$

in the Higgs potential.

The charged gauge bosons $W_{L,R}^\pm$ acquire mass by eating two colourless, charged would-be Goldstone bosons (let's call them G_R^\pm and G_L^\pm) which are linear combinations of $\chi_{L,R}^{4,-\frac{1}{2}}$, $\phi^{\frac{1}{2},\frac{1}{2}}$ and $\phi^{-\frac{1}{2},-\frac{1}{2}}$, leaving behind two physical charged Higgs (which we will call $H_{1,2}^\pm$). The fields $\chi_{L,R}^{4,-\frac{1}{2}}$ appearing in Fig. 3 are linear combination of these would-be Goldstone bosons and physical Higgses. We shall work out the linear combinations of $G_{L,R}^\pm$ and $H_{1,2}^\pm$ in $\chi_{L,R}^{4,-\frac{1}{2}}$ so that the Dirac mass arising from these χ -interactions can be calculated.

The Goldstone bosons associated with each spontaneously broken symmetry are given by

$$G = \Phi^T T^a \lambda_a, \tag{42}$$

where Φ are the Higgs scalars of the theory, T^a the generators of the broken symmetries and λ_a the vacua. Utilising Eq. (42), the would-be Goldstone bosons G_L^\pm and G_R^\pm can be identified by taking T^a as the charged $SU(2)_{L,R}$ generators, τ_\pm . The two states which are orthogonal to G_R^\pm and G_L^\pm will be related to the physical Higgs $H_{1,2}^\pm$ with masses denoted by M_{H_1,H_2} . We will first work in the limit $u_1 \rightarrow 0$ since we expect $u_1 \ll u_2$ (or $u_2 \ll u_1$, which is analogous to $u_1 \ll u_2$ in the following analysis). In this limit it is possible to show that (see Appendix) the weak eigenstates are related to $G_{L,R}^\pm, H_{1,2}^\pm$ via the unitary matrix U_g as

$$\begin{pmatrix} \chi_R^{4,-\frac{1}{2}} \\ \chi_L^{4,-\frac{1}{2}} \\ \phi^{\frac{1}{2},\frac{1}{2}*} \\ \phi^{-\frac{1}{2},-\frac{1}{2}} \end{pmatrix} = U_g \begin{pmatrix} G_R^- \\ G_L^- \\ H_1^- \\ H_2^- \end{pmatrix}, \quad (43)$$

where the matrix U_g is (in the limit $u_1 \rightarrow 0$)

$$U_g = \begin{pmatrix} \frac{w_R}{N_g} & 0 & \frac{u_2^2/w_R}{N_1} & 0 \\ 0 & \frac{w_L}{N_L} & 0 & \frac{-u_2^2/w_L}{N_2} \\ \frac{-u_2}{N_g} & 0 & \frac{u_2}{N_1} & 0 \\ 0 & \frac{u_2}{N_L} & 0 & \frac{u_2}{N_2} \end{pmatrix} \equiv \begin{pmatrix} U_{11} & U_{12} & U_{13} & U_{14} \\ U_{21} & U_{22} & U_{23} & U_{24} \\ U_{31} & U_{32} & U_{33} & U_{34} \\ U_{41} & U_{42} & U_{43} & U_{44} \end{pmatrix}, \quad (44)$$

with normalisation constants

$$\begin{aligned} N_g^2 &= w_R^2 + u_2^2, \quad N_L^2 = w_L^2 + u_2^2, \\ N_1^2 &= u_2^2 \left[1 + \left(\frac{u_2}{w_R} \right)^2 \right], \quad N_2^2 = u_2^2 \left[1 + \left(\frac{u_2}{w_L} \right)^2 \right]. \end{aligned} \quad (45)$$

Referring to Eqs. (43), (44), we observe that

$$\begin{aligned} \chi_R^{4,-\frac{1}{2}} &= \frac{w_R}{\sqrt{w_R^2 + u_2^2}} G_R^- + \frac{u_2}{\sqrt{w_R^2 + u_2^2}} H_1^-, \\ \chi_L^{4,-\frac{1}{2}} &= \frac{w_L}{\sqrt{w_L^2 + u_2^2}} G_L^- - \frac{u_2}{\sqrt{w_L^2 + u_2^2}} H_2^-. \end{aligned} \quad (46)$$

Thus it is clear that the χ -loop correction vanishes in the limit $u_1 \rightarrow 0$. Self consistency implies that

$$\lim_{\substack{u_1 \rightarrow 0 \\ u_2 \neq 0}} V_{3\langle\phi\rangle} = \lim_{\substack{u_2 \rightarrow 0 \\ u_1 \neq 0}} V_{3\langle\phi\rangle} = 0, \quad (47)$$

which we also prove in the Appendix. In short, the χ -loop contribution to the neutrino Dirac mass vanishes in the limit $u_1 \rightarrow 0$ (or analogously $u_2 \rightarrow 0$). Recall that the gauge contribution to Dirac mass also vanishes in this limit. The expected hierarchy $u_1 \ll u_2$ (or $u_2 \ll u_1$) thus ensures a small gauge *and* scalar contribution to the neutrino Dirac mass.

We now investigate the case of small $u_1 \neq 0$ (with $u_1 \ll u_2$). In this case we can treat the u_1 term as a perturbation that induces small mass mixing term $V_{3\langle\phi\rangle}$ that will couple $\chi_R^{4,-\frac{1}{2}}$ to $\chi_L^{4,-\frac{1}{2}}$, thus leading to neutrino Dirac masses. This argument also holds true if we interchange $u_1 \leftrightarrow u_2$. Indexing the would-be Goldstone bosons and physical Higgs fields as

$$S_a^T = (G_R^-, G_L^-, H_1^-, H_2^-), \quad a = 1, 2, 3, 4, \quad (48)$$

we can write the linear combination of $G_{L,R}^-$ and $H_{1,2}^-$ in $\chi_{L,R}^{4,-\frac{1}{2}}$ compactly as

$$\chi_R^{4,-\frac{1}{2}} = \sum_{a'=1,3} U_{1a'} S_{a'}, \quad \chi_L^{4,-\frac{1}{2}} = \sum_{b=2,4} U_{2b} S_b. \quad (49)$$

The explicit expression of $U_{1a'}, U_{2b}$ can be read off directly from U_g in Eq. (44). The mass correction in Fig. 3 is now a summation of all the contributions from the approximate mass eigenstates diagrams. Now we could evaluate the Feynman diagram in Fig. 3 by treating the cross insertion as a perturbation that gives rise to a vertex factor $m_{3(\phi)}^2 = -(Mu_1 + M'u_2)$. In the special case of decoupled generations, the mass correction is calculated to be (for first generation)

$$m_D = k_\chi m_e, \quad (50)$$

with

$$k_\chi = \frac{M_E^2}{16\pi^2 w_L w_R} A, \quad (51)$$

where

$$A = \sum_{a',b} A_{a'b} U_{1a'} U_{2b},$$

$$A_{a'b} = \left(\frac{Mu_1 + M'u_2}{M_{S_{a'}}^2 - M_E^2} \right) \left[\frac{M_{S_{a'}}^2 \ln\left(\frac{M_{S_b}^2}{M_{S_{a'}}^2}\right)}{M_{S_b}^2 - M_{S_{a'}}^2} - \frac{M_E^2 \ln\left(\frac{M_{S_b}^2}{M_E^2}\right)}{M_{S_b}^2 - M_E^2} \right]. \quad (52)$$

This quantity A can be greatly simplified in the limit $w_R^2 \gg u_2^2 \gg w_L^2, u_1^2$. In this limit G_R^- and H_2^- will dominate the loop:

$$A \approx \left(\frac{Mu_1 + M'u_2}{M_{W_R}^2 - M_E^2} \right) \left[\frac{M_{H_2}^2 \ln\left(\frac{M_{H_2}^2}{M_{W_R}^2}\right)}{M_{H_2}^2 - M_{W_R}^2} - \frac{M_E^2 \ln\left(\frac{M_{W_R}^2}{M_E^2}\right)}{M_{W_R}^2 - M_E^2} \right], \quad (53)$$

where we have set the mass of G_R^\pm to the mass of M_{W_R} since we are working in the t'Hooft-Feynman gauge. Putting in reasonable limits for the parameters ($M_{W_R} \gtrsim 0.5$ TeV, 50 GeV $< M_E \lesssim 10$ TeV, 1 GeV $< w_L < 200$ GeV), we find

$$\frac{u_1 u_2 M_E^4}{w_L w_R M_{W_R}^4} \lesssim k_\chi \lesssim \frac{u_1 u_2}{w_L w_R}. \quad (54)$$

Thus we can now constrain the relative contribution of the gauge and χ -loop diagrams. We find that

$$\frac{M_E^4}{M_{W_R}^4} \frac{w_R}{w_L} \lesssim \frac{k_\chi}{k_g} \lesssim \frac{w_R}{w_L}. \quad (55)$$

Using $\frac{M_E}{M_{W_R}} \gtrsim 10^{-2}$ and $10 \lesssim \frac{w_R}{w_L} \lesssim 10^4$, we have

$$10^{-7} \lesssim \frac{k_\chi}{k_g} \lesssim 10^4. \quad (56)$$

Thus there is a range of parameters where gauge loop dominates ($k_g \gg k_\chi$) and range of parameters where χ -loop dominates ($k_g \ll k_\chi$). There is also a troublesome intermediate region with $k_g \approx k_\chi$ which we will for the most part ignore.

V. $\tilde{\nu}_L - \tilde{\nu}_R$ MIXING IN DECOUPLED GENERATIONS

Having derived the various contributions to the neutral lepton mass matrix \mathbf{M} , we now examine the scenario where we assume that the mixing between generations is approximately negligible. Referring to the tree level mass matrix \mathbf{M} of Eq. (24), $\tilde{\nu}_R$ gains a Majorana mass from its mixing with the E leptons while $\tilde{\nu}_L$ is massless at tree level. Including the 1-loop mass corrections, the mass matrix \mathbf{M} is

$$\mathbf{M} = \begin{pmatrix} m_M & m_D & m_{\nu E} & 0 \\ m_D^\dagger & 0 & Y_R M_u Y_L^\dagger U & M_l V \\ m_{\nu E}^\dagger & (Y_R M_u Y_L^\dagger U)^\dagger & 0 & -M_E \\ 0 & (M_l V)^\dagger & -M_E & 0 \end{pmatrix}. \quad (57)$$

The neutrinos (both left-handed and right-handed ones) will approximately decouple from the E leptons since the latter are much heavier (recall that $M_E \gtrsim 45$ GeV from Z^0 width). The effective Lagrangian density for the mass matrix of the neutrinos after decoupling from the E leptons is

$$\mathcal{L}_{eff} = \frac{1}{2} \left(\overline{\tilde{\nu}_L} \overline{(\tilde{\nu}_R)^c} \right) M_\nu \begin{pmatrix} (\tilde{\nu}_L)^c \\ \tilde{\nu}_R \end{pmatrix} + \text{H. c.}, \quad (58)$$

where the matrix M_ν is as given by

$$M_\nu \simeq \begin{pmatrix} m_M & m'_D \\ (m'_D)^\dagger & M_R \end{pmatrix}, \quad (59)$$

with

$$m'_D = m_D + m_{\nu E} M_E^{-1} V^\dagger M_l. \quad (60)$$

M_R is given earlier in Eq. (28). In the see-saw limit where the eigenvalues of M_R are much larger than the eigenvalues of m'_D , Eq. (58) becomes

$$\mathcal{L}^{see-saw} \simeq \frac{1}{2} \overline{\tilde{\nu}_L} m_L (\tilde{\nu}_L)^c + \frac{1}{2} \overline{(\tilde{\nu}_R)^c} M_R \tilde{\nu}_R + \text{H.c.}, \quad (61)$$

where

$$\begin{aligned} m_L &\simeq m_M - m'_D M_R^{-1} (m'_D)^\dagger \\ &= m_M - V_L \begin{pmatrix} m_{11} & 0 & 0 \\ 0 & m_{22} & 0 \\ 0 & 0 & m_{33} \end{pmatrix} V_R^\dagger U_R^* \begin{pmatrix} M_1 & 0 & 0 \\ 0 & M_2 & 0 \\ 0 & 0 & M_3 \end{pmatrix}^{-1} \times \\ &\quad U_R^\dagger V_R^* \begin{pmatrix} m_{11} & 0 & 0 \\ 0 & m_{22} & 0 \\ 0 & 0 & m_{33} \end{pmatrix} V_L^T, \end{aligned} \quad (62)$$

with m_{ii} and M_i ($i = 1, 2, 3$) as the eigen masses of the mass matrices m_D and M_R respectively. In Eq. (62) we have assumed that the matrices M_R and m'_D are diagonalised with

$$M_R = U_R \begin{pmatrix} M_1 & 0 & 0 \\ 0 & M_2 & 0 \\ 0 & 0 & M_3 \end{pmatrix} U_R^\dagger, \quad m'_D = V_L \begin{pmatrix} m_{11} & 0 & 0 \\ 0 & m_{22} & 0 \\ 0 & 0 & m_{33} \end{pmatrix} V_R^\dagger. \quad (63)$$

Generically m_M is always tiny in comparison to the other contributions to m_L in all generations and shall be dropped hereafter.

In the case of decoupled generations the mixing angle between $\tilde{\nu}_L$ with $\tilde{\nu}_R$ can be determined from the matrix M_ν :

$$\tan 2\theta_\nu = -\frac{2m'_D}{M_R}. \quad (64)$$

The eigen masses of M_ν are

$$\frac{1}{2} \left(M_R \pm \sqrt{M_R^2 + 4m'^2_D} \right) = \frac{M_R}{2} \left(1 \pm \frac{1}{\cos 2\theta_\nu} \right) \quad (65)$$

and the mass squared difference is simply

$$\delta m_\nu^2 = \frac{M_R^2}{\cos 2\theta_\nu} = \left(\frac{2m_l m_{q_u}}{M_E} \right)^2 \frac{1}{\cos 2\theta_\nu}. \quad (66)$$

Under the assumption of decoupled generations, the only way to solve atmospheric neutrino anomaly is via $\tilde{\nu}_{\mu L} \rightarrow (\tilde{\nu}_{\mu R})^c$ oscillations. However, since experimentally we know that $\delta m_{atm}^2 \lesssim 10^{-2} \text{ eV}^2$, $\sin^2 2\theta_{atm} \gtrsim 0.8$, this implies

$$M_E = \frac{2m_{q_u} m_l}{\sqrt{\delta m_{atm}^2 \cos 2\theta_{atm}}} \gtrsim 70 \text{ TeV} \quad (67)$$

even with the lowest possible fermion masses $m_{q_u} = m_u, m_l = m_e$. Thus it is not possible to solve atmospheric neutrino anomaly with decoupled generations while keeping the symmetry breaking scale in the interesting range \lesssim few TeV. The above result applies to both cases where m'_D is dominated by the gauge loop or by the χ -loop.

VI. MIRROR SYMMETRISATION OF THE ALTERNATIVE 422 MODEL

As concluded in the last section, decoupled generations cannot accommodate the atmospheric neutrino anomaly within our assumption of a low 422 symmetry breaking scale \lesssim few TeV. Nevertheless, we can still have near maximal active-sterile oscillations at the TeV scale if we mirror symmetrise the alternative 422 model in the spirit of the Exact Parity Model (EPM) [34]. These models allows parity to be an unbroken symmetry of nature which it turns out offers a framework to understand the dark matter, neutrino anomalies and various other puzzles. (For a review of the evidence see [35].) It is well known that in mirror matter models maximal mixing occurs naturally because of the unbroken parity symmetry. In the ‘mirror symmetric alternative 422 model’, $\tilde{\nu}_L$ will oscillate maximally to its parity partner $(\tilde{\nu}'_R)^c$. Mirror symmetrisation can thus provide a mechanism to obtain

maximal mixing whereas the naturally tiny masses (hence mass squared difference) of the neutrinos are radiatively generated and naturally small in this TeV scale model.

In the mirror symmetric alternative 422 model, the symmetry group is extended to $SU(4) \otimes SU(2)_L \otimes SU(2)_R \otimes SU(4)' \otimes SU(2)'_L \otimes SU(2)'_R$. Each family has a mirror partner, which we denote with a prime. Considering $\tilde{\nu}_L$ and $\tilde{\nu}_R$, $\tilde{\nu}'_R$ and $\tilde{\nu}'_L$ will be included in the particle content enabling parity to be an unbroken symmetry. Under the parity transformation, $\tilde{\nu}_L \leftrightarrow \gamma_0 \tilde{\nu}'_R$, $\tilde{\nu}_R \leftrightarrow \gamma_0 \tilde{\nu}'_L$ (as well as $x \rightarrow -x$, of course). The see-saw Langrangian density of Eq. (61) becomes

$$\mathcal{L}^{see-saw} = \frac{1}{2} \begin{pmatrix} \overline{\tilde{\nu}_L} & \overline{(\tilde{\nu}'_R)^c} & \overline{(\tilde{\nu}_R)^c} & \overline{\tilde{\nu}'_L} \end{pmatrix} M'_\nu \begin{pmatrix} (\tilde{\nu}_L)^c \\ \tilde{\nu}'_R \\ \tilde{\nu}_R \\ (\tilde{\nu}'_L)^c \end{pmatrix} + \text{H.c.}, \quad (68)$$

where

$$M'_\nu = \begin{pmatrix} 0 & m' & m'_D & 0 \\ m' & 0 & 0 & m'_D \\ (m'_D)^\dagger & 0 & M_R & 0 \\ 0 & (m'_D)^\dagger & 0 & M_R \end{pmatrix}. \quad (69)$$

m' is a parity invariant mass mixing term that mixes the ordinary neutrinos with the mirror neutrinos. In the minimal mirror matter 422 model, i.e. with only the Higgs fields ϕ, χ_L, χ_R and ϕ', χ'_L, χ'_R , there is no mirror-ordinary mixing Yukawa coupling to generate m' . This is quite unlike the case of the EPM model where ordinary-mirror Yukawa coupling $\overline{(\tilde{\nu}'_L)^c} \phi \tilde{\nu}_L$ exists because $\tilde{\nu}_R$ and its parity partner $\tilde{\nu}'_L$ are gauge singlets. One could consider the mirror-ordinary mass mixing term as a dimension-five unrenormalisable bare mass term $\lambda_0 \overline{f'_R} \phi' f_L \phi / M_h$ so that the mirror symmetric alternative 422 model becomes effectively a remnant resulting from the breakdown of some unknown physics at a much higher scale M_h .

Alternatively, the required mirror-ordinary mass mixing term can be generated if an additional Higgs scalar $\rho^{\alpha\beta, \alpha'\beta'} \sim (2, 2)(2', 2')$ exists. The gauge invariant Yukawa coupling

$$\mathcal{L}_\rho = \lambda_5 \overline{f_L} \rho \tau_2 f'_R + \lambda_6 \overline{f_L} \rho^c \tau_2 f'_R + \text{H.c.} \quad (70)$$

will generate a mirror-ordinary mass mixing term as ρ develops a VEV. Because ρ can couple to $\phi\phi'$ in Higgs potential it can easily gain a VEV in the right orientation.

To see this more transparently, let's take a look at the part of Higgs potential containing only the scalar field ρ ,

$$V(\rho) = M_\rho^2 \rho^\dagger \rho + m_\rho \phi'^\dagger \phi^\dagger \rho + m'_\rho (\rho^c)^\dagger \phi \phi' + \mathcal{O}(\rho^3, \rho^4) + \text{H.c.} \quad (71)$$

As ϕ, ϕ' develop VEVs at $\langle \phi \rangle = \langle \phi' \rangle = \begin{pmatrix} 0 & u_2 \\ u_1 & 0 \end{pmatrix}$, the trilinear term will induce a linear term in ρ . Because of this, minimising $V(\rho)$ with respect to ρ^\dagger

$$\frac{\partial V}{\partial \rho^\dagger} = M_\rho^2 \rho + m_\rho \langle \phi \rangle \langle \phi' \rangle + m'_\rho \langle \phi'^c \rangle \langle \phi^c \rangle = 0 \quad (72)$$

will induce the VEVs

$$\langle \rho \rangle = -\frac{m_\rho \langle \phi \rangle \langle \phi' \rangle + m'_\rho \langle \phi'^c \rangle \langle \phi^c \rangle}{M_\rho^2} \quad (73)$$

to the components of $\rho^{\alpha\beta, \alpha'\beta'}$. The VEV for the component

$$\langle \rho \rangle^{(12, 2'1')} = \langle \rho^c \rangle^{(12, 2'1')} = -\frac{(m_\rho + m'_\rho) u_1 u_2}{M_\rho^2} \quad (74)$$

will generate the desired ordinary-mirror mass mixing term in \mathcal{L}_ρ :

$$\mathcal{L}_\rho = \overline{\tilde{\nu}_L} m' \tilde{\nu}'_R + \text{H.c.}, \quad (75)$$

where

$$m' = -\lambda_5 \langle \rho \rangle^{(12, 2'1')} - \lambda_6 \langle \rho^c \rangle^{(12, 2'1')} = \frac{u_1 u_2 (m_\rho + m'_\rho)}{M_\rho^2} (\lambda_5 + \lambda_6). \quad (76)$$

In any case the mirror-ordinary mass mixing term m' is still a free parameter of the theory. In the see-saw limit $\tilde{\nu}_L, (\tilde{\nu}'_R)^c$ decouple from $\tilde{\nu}'_L, (\tilde{\nu}_R)^c$ in Eq. (68) and the Lagrangian density of light neutrinos is given by

$$\mathcal{L}_\nu'' = \frac{1}{2} \left(\overline{\tilde{\nu}_L} \quad \overline{(\tilde{\nu}'_R)^c} \right) M'' \begin{pmatrix} (\tilde{\nu}_L)^c \\ \tilde{\nu}'_R \end{pmatrix} + \text{H.c.}, \quad (77)$$

where

$$M'' = \begin{pmatrix} -m'_D M_R^{-1} (m'_D)^\dagger & m' \\ m' & -m'_D M_R^{-1} (m'_D)^\dagger \end{pmatrix}. \quad (78)$$

The mass matrix M'' in Eq. (78) describes maximal $\tilde{\nu}_L \rightarrow (\tilde{\nu}'_R)^c$ oscillations with eigen masses

$$m_\pm = -m'_D M_R^{-1} (m'_D)^\dagger \pm m'. \quad (79)$$

In the limit of small intergenerational mixing the mass squared difference is simply

$$\delta m_{\mp}^2 = \frac{4m' m_D^2}{M_R} = \frac{2m' m_l M_{E_i} S^2 \eta^2}{m_{qu}}. \quad (80)$$

δm_{\pm}^2 can be identified as δm_{atm}^2 (second generation) and δm_{solar}^2 (first generation) with maximal oscillation solutions, thereby explaining the atmospheric and solar neutrino anomalies. If small intergenerational mixing (parametrised by θ and ϕ) between the first and second generations is included, the LSND experiment δm_{LSND}^2 can be identified with

$$\delta m_{LSND}^2 \equiv |\delta m_{\nu_{e+}, \nu_{\mu+}}^2| \equiv |m_{\nu_{e+}}^2 - m_{\nu_{\mu+}}^2| \quad (81)$$

and

$$(\sin 2\theta + \sin 2\phi)^2 \sim 3 \times 10^{-2} - 10^{-3}. \quad (82)$$

Thus, the mirror symmetrised extension of the alternative 422 model can explain all the three neutrino anomalies without any physics beyond the TeV scale. The alternative 422 model provides the neutrino masses while mirror symmetrising it provides the maximal mixing between each ordinary and mirror neutrino flavour.

VII. MIXING BETWEEN GENERATIONS: NEUTRINO MASS DOMINATED BY GAUGE INTERACTIONS

In the previous two sections we have examined the case where the mixing between generations was small. Under this assumption the minimal alternative 422 model could not accommodate the large mixing required to explain the atmospheric or solar neutrino problems. However we also shown that the mirror symmetrised extension could explain all three neutrino anomalies. We now return to the minimal alternative 422 model and examine the alternative case where mixing between generations is large. From the discussion in the previous sections, recall that there are two different ways in which neutrino masses are generated in the model, namely via the gauge interactions and via the (scalar) χ -interactions. In either case, we see that the Dirac masses are proportional to the charged lepton masses m_l [see Eq. (32), (50)]. The proportional constants k_χ and k_g are poorly constrained however. Our ignorance of their relative strength does not permit us to tell which mechanism is the dominating one. Though it remains a possibility that both contributions may be equally contributive, we shall not treat this general scenario to avoid complications. We will focus our attention only to the limiting case where the gauge interactions are assumed to dominate over the scalar interactions, i.e. $k_g \gg k_\chi$.

A. Two generations maximal mixing and ‘lop-sided’ M_R

In this subsection, we shall analyse the limiting case where the radiative contribution to the neutrino mass from gauge interactions dominates the contribution due to the scalar interactions, i.e. $k_g \gg k_\chi$. Our strategy is to look for a mechanism in the 2-3 sector that provides a near maximal $\tilde{\nu}_{\mu L} \rightarrow \tilde{\nu}_{\tau L}$ oscillation solution to atmospheric neutrino anomaly. We then generalise it to the case of three generations.

Recall that the effective mass matrix for the light neutrinos is given by m_L [see Eq. (62)]. Knowledge of m_L allows us to work out the mixing angles and δm^2 , and to make contact with the neutrino experiments. In general, to calculate m_L we require knowledge of the Yukawa coupling matrices $\lambda_1, \dots, \lambda_4$. Our purpose here is to identify simple forms of $\lambda_1, \dots, \lambda_4$ which enable the model to accommodate the neutrino data. Let us first look at the special case of just the 2-3 sector. As discussed in Ref. [33], we can obtain maximal $\tilde{\nu}_{\mu L} \rightarrow \tilde{\nu}_{\tau L}$ oscillations if m'_D is approximately diagonal and M_R being ‘lop sided’, meaning that the off diagonal elements are much larger than the diagonal elements of the 2-3 mass matrix.

The (tree level) two generations mass matrix M_R in the 2-3 sector, which we parametrise by

$$M_{R2} = \begin{pmatrix} r_{22} & r_{23} \\ r_{23} & r_{33} \end{pmatrix} \quad (83)$$

can be easily worked out from Eq. (28). Note that the form of M_{R2} is intimately related to the Yukawa couplings λ_1 as well as the right-handed CKM-type matrix Y_R . On the other hand, quite independently, the radiative correction to the neutrino mass m'_D can be read off directly from Eq. (60). Cross generational mixing of the Dirac masses is possible due to

the dependence of the matrix V . However, in the limiting case of diagonal V , the matrix $m_{\nu E}$, and thus m'_D , also becomes diagonal. In this case we can approximate m'_D by m_D ***. The Dirac masses of $m'_D \sim m_D$, namely m_{22}, m_{33} , are simply given by Eq. (34), with $m_l = m_\mu, m_\tau$ respectively.

Let us parametrise the unitary matrices [as introduced in Eq. (19)] as

$$U = \begin{pmatrix} \cos \theta_u & -\sin \theta_u \\ \sin \theta_u & \cos \theta_u \end{pmatrix}, V = \begin{pmatrix} \cos \theta_v & -\sin \theta_v \\ \sin \theta_v & \cos \theta_v \end{pmatrix}, Y_R = \begin{pmatrix} \cos \theta_y & -\sin \theta_y \\ \sin \theta_y & \cos \theta_y \end{pmatrix}. \quad (84)$$

The simplest way that we have found to obtain lop-sided M_R in our scheme (modulo certain ‘permutations’ which we will discuss later) is to note that when λ_1 is approximately diagonal (i.e. $\theta_{u,v}$ small)^{†††}, then

$$\lim_{\theta_{u,v} \rightarrow 0} M_{R2} = \begin{pmatrix} \frac{2 \cos \theta_y m_\mu m_c}{M_{E2}} & \frac{\sin \theta_y m_\mu m_c - \frac{m_\tau m_t}{M_{E3}}}{M_{E2}} \\ \frac{\sin \theta_y m_\mu m_c - \frac{m_\tau m_t}{M_{E3}}}{M_{E2}} & \frac{2 \cos \theta_y m_\tau m_t}{M_{E3}} \end{pmatrix}. \quad (85)$$

If we let M_{R2} be diagonalised by the unitary matrix

$$U_{R2} = \begin{pmatrix} \cos \theta_R & -\sin \theta_R \\ \sin \theta_R & \cos \theta_R \end{pmatrix}, \quad (86)$$

we find that the mixing angle θ_R behaves like

$$\lim_{\theta_{u,v} \rightarrow 0} \tan 2\theta_R = -\frac{m_\tau m_t / M_{E3}}{\left(\frac{m_\tau m_\mu}{M_{E2}} - \frac{m_\tau m_t}{M_{E3}}\right) \cos \theta_y}. \quad (87)$$

This mean that, assuming no accidental cancellation, we will obtain $|\tan 2\theta_R| \gg 1$ in the limit

$$\theta_{u,v} \rightarrow 0, \theta_y \rightarrow \frac{\pi}{2}, \quad (88)$$

with a pair of approximately degenerate eigen masses

$$M_{2,3} \simeq \mp \left(\frac{m_\mu m_c}{M_{E2}} - \frac{m_\tau m_t}{M_{E3}} \right) \equiv \mp m_{\nu R}. \quad (89)$$

Since m'_D is kept diagonal due to the vanishing θ_v , therefore maximal mixing in the left-handed neutrinos (2-3 sector) is realised. This can be seen from the effective mass matrix m_L of Eq. (62):

***In the case where the radiative correction is dominated by the gauge interactions $m_{\nu E}$ will contribute to m'_D [see Eq. (60)]. In the special case of decoupled generations, $m'_D = m_D + m_{\nu E} m_l / M_{E_i}$. Ref. [9] established the estimation of $m_D \sim m_{\nu E} m_l / M_{E_i}$. Assuming no accidental cancellation, we could approximate $m'_D \sim m_D$.

^{†††} For simplicity we have set the CKM matrix $Y_L = \mathbf{I}$.

$$m_L \rightarrow \begin{pmatrix} 0 & 1 \\ 1 & 0 \end{pmatrix} \frac{m_{22}m_{33}}{m_{\nu R}}. \quad (90)$$

The effective mass matrix Eq. (90) indicates that, in the presence of small intergenerational mixing, the left-handed active neutrinos $\tilde{\nu}_{\mu L}, \tilde{\nu}_{\tau L}$ are approximate maximal mixture of almost degenerate mass eigenstates. We denote these eigen masses as

$$m_2, m_3 = \frac{\pm \eta^2 S^2}{\left(\frac{m_c}{m_\tau M_{E_2}} - \frac{m_t}{m_\mu M_{E_3}}\right)}. \quad (91)$$

In the case where the limits of Eq. (88) are only approximate, the diagonal entries in M_{R2} (and hence m_L) shall in effect be replaced by some tiny values ϵ instead. It is natural to conceive that ϵ could split the eigen mass degeneracy to an order of $10^{-3} \text{ eV}^2 \lesssim |\delta m_{atm}^2| \equiv |m_3^2 - m_2^2| \lesssim 10^{-2} \text{ eV}^2$. However, if this splitting is to be natural, the size of $\delta m_{3,2}^2 \equiv m_3^2 - m_2^2$ must be smaller than m_2^2, m_3^2 themselves, i.e.,

$$m_3^2, m_2^2 \gg 10^{-2} \text{ eV}^2. \quad (92)$$

Estimating $m_{2,3}^2$ [using the range of S from Eq. (36)],

$$m_{2,3}^2 \approx M_{E_3}^2 \left(\frac{m_\mu}{m_t}\right)^2 S^4 \eta^4 \lesssim 10^{-7} \left(\frac{M_{E_3}}{\text{TeV}}\right)^2 \text{ eV}^2. \quad (93)$$

Thus, we see that although near maximal $\tilde{\nu}_{\mu L} \rightarrow \tilde{\nu}_{\tau L}$ oscillations are achieved via the ansatz of Eq. (88) the δm^2 is not in natural compatibility with δm_{atm}^2 in this particular situation. This means that maximal oscillation solution to atmospheric neutrino anomaly is not accommodated in this case. However we will show later that a permutation on the up-type quark masses in m_i could be performed to obtain compatibility with the consistency requirement of Eq. (92). It is more convenient to discuss how the permutation (and its rationale) of the up-type quark masses could obtain a compatible range of δm^2 between this scheme and the experimental values by including the first generation neutrino into the picture. We shall do so in the following subsection.

Before we proceed to the three generations case, it is worth to comment on the form taken by Y_R^\dagger under the ansatz of Eq. (88). Since m_D is approximately diagonal under this ansatz, near maximal $\tilde{\nu}_{\mu L} \rightarrow \tilde{\nu}_{\tau L}$ oscillations should originate from M_{R2} of the right-handed neutrino sector, which is in turn related to the form of Y_R^\dagger and the mass matrix λ_1 . In the limit of this ansatz, Y_R^\dagger is off-diagonal in the 2-3 sector (assuming that the first generation is approximately decoupled from the 2-3 sector),

$$Y_R^\dagger \sim \begin{pmatrix} 1 & 0 & 0 \\ 0 & 0 & 1 \\ 0 & 1 & 0 \end{pmatrix}. \quad (94)$$

If we assume a left-right similarity so that

$$K_R \sim K_L \sim \mathbf{I}, \quad (95)$$

then this means that $K' \equiv Y_R^\dagger K_R^\dagger$ also has the form

$$K' \sim \begin{pmatrix} 1 & 0 & 0 \\ 0 & 0 & 1 \\ 0 & 1 & 0 \end{pmatrix} = Y^\dagger. \quad (96)$$

Recall that, as discussed in detail by Ref. [5,9], the $SU(4)$ gauge interactions involving the coloured gauge bosons W'_μ

$$\mathcal{L} = \frac{g_s}{\sqrt{2}} \overline{D_R} W'_\mu \gamma^\mu K' l_R + \text{H. c.} \quad (97)$$

could mediate lepto-quark transitions. In Ref. [5,9] it was shown that K' must be non-diagonal to avoid contributions from $K^0 \rightarrow \mu^\pm e^\mp$ decays. In that case the primary constraint on the $SU(4)$ symmetry breaking scale $M_{W'}$ is from rare B_0 decays, $B_0 \rightarrow \mu^\pm e^\mp, \tau^\pm e^\mp$ and $\tau^\pm \mu^\mp$, depending on the forms of K' , resulting in the low symmetry breaking scale of $\sim \text{TeV}$. Specifically, in order for the TeV symmetry breaking scale to occur, K' have to be in certain forms that will suppress the rare decays $K_L \rightarrow \mu^\pm e^\mp$. In fact Ref. [9] pointed that there are only 4 possible (approximate) forms for K' that are consistent with the TeV SSB scale:

$$\begin{aligned} K'_1 &= \begin{pmatrix} 0 & 0 & 1 \\ \cos \alpha & \sin \alpha & 0 \\ -\sin \alpha & \cos \alpha & 0 \end{pmatrix}, & K'_2 &= \begin{pmatrix} \cos \beta & \sin \beta & 0 \\ 0 & 0 & 1 \\ -\sin \beta & \cos \beta & 0 \end{pmatrix}, \\ K'_3 &= \begin{pmatrix} \cos \gamma & 0 & \sin \gamma \\ -\sin \gamma & 0 & \cos \gamma \\ 0 & 1 & 0 \end{pmatrix}, & K'_4 &= \begin{pmatrix} 0 & \cos \delta & \sin \delta \\ 0 & -\sin \delta & \cos \delta \\ 1 & 0 & 0 \end{pmatrix}. \end{aligned} \quad (98)$$

Note that Eq. (96) is a special case of these forms, namely,

$$K'_2(\beta = 0) = K'_3(\gamma = 0). \quad (99)$$

Eq. (95) amounts to suggesting that non-diagonal K' (required for low symmetry breaking) and non-diagonal Y_R^\dagger (required to obtain maximal $\tilde{\nu}_{\mu L} \rightarrow \tilde{\nu}_{\tau L}$ oscillations) may have a common origin. For example, if we make the ansatz that λ_3, λ_4 takes the approximate form

$$\lambda_3 \sim \begin{pmatrix} \times & 0 & 0 \\ 0 & 0 & \times \\ 0 & \times & 0 \end{pmatrix}, \quad \lambda_4 \sim \begin{pmatrix} \times & 0 & 0 \\ 0 & 0 & \times \\ 0 & \times & 0 \end{pmatrix}, \quad (100)$$

with the other 2 Yukawas $\{\lambda_1, \lambda_2\}$ approximately diagonal, then this will simultaneously lead to Eq. (94) and (96), hence the low symmetry breaking scale ($\sim \text{few TeV}$) and near maximal $\tilde{\nu}_{\mu L} \rightarrow \tilde{\nu}_{\tau L}$ oscillations.

B. Permutation of up-type quark masses and three generations mixing

In this subsection we will include the first generation neutrino into the picture under the assumption that the intergenerational mixing between the first and the 2-3 sector is small. In such a scenario m_L will take the approximate form

$$m_L \approx \begin{pmatrix} -\frac{m_{11}^2}{M_1} & 0 & 0 \\ 0 & 0 & \frac{m_{22}m_{33}}{m_{\nu_R}} \\ 0 & \frac{m_{22}m_{33}}{m_{\nu_R}} & 0 \end{pmatrix} \quad (101)$$

which leads to a pair of almost degenerate eigen masses m_2, m_3 in the 2-3 sector that is separated from eigen mass

$$m_1 = -\frac{m_{11}^2}{M_1} = -\frac{m_e M_{E1} \eta^2 S^2}{2m_u} \text{ eV} \quad (102)$$

with a distinct gap. The near maximal oscillation solution for atmospheric neutrino anomaly corresponds to a near degenerate pair of eigen masses m_2, m_3 . It is obvious that to include the first generation neutrino to solve the solar neutrino anomaly (which involves a much smaller $\delta m^2 \lesssim 10^{-3} \text{ eV}^2$ required by all oscillation solutions) the first generation neutrino mass will have to be very nearly degenerate with the other two neutrino masses, which is quite unnatural. Thus we conclude that the gauge loop mechanism seems to explain the LSND data more readily than the solar neutrino anomaly. The gap $\delta m_{1,3}^2 \approx \delta m_{1,2}^2$ can then be identified with the LSND measurement, $0.2 \text{ eV}^2 \lesssim \delta m_{LSND}^2 \lesssim 3 \text{ eV}^2$ ^{†††}.

In the case of two generations discussed in the previous subsection, the form of the matrix $K' \equiv K'_2(\beta = 0) = K'_3(\gamma = 0)$ in Eq. (96) leads to the scale of $m_{2,3}^2$ that are incompatible to Eq. (92). However, this result corresponds to only one specific form of K' in Eq. (98). In general, the other forms of K' in Eq. (98) could also lead to maximal neutrino oscillations that are consistent with TeV scale SSB, assuming that $Y_R^\dagger = K'$ holds. Essentially there are only 4 special forms of K' that are of our interest. The case of $K' \equiv K'_2(\beta = 0) = K'_3(\gamma = 0)$ has been shown to be incompatible with Eq. (92). We will investigate the other three forms of K' in turns, namely (a) $K'_4(\delta = 0) = K'_2(\beta = \frac{\pi}{2})$, (b) $K'_1(\alpha = 0) = K'_3(\gamma = \frac{\pi}{2})$ and (c) $K'_4(\alpha = \frac{\pi}{2}) = K'_4(\delta = \frac{\pi}{2})$.

To find out how these three different forms of K' can also lead to maximal mixing in the 2-3 sector, we will use the constraint that the lop-sided form of M_R , and thus maximal $\tilde{\nu}_{\mu L} \rightarrow \tilde{\nu}_{\tau L}$ oscillations, is preserved when Y_R^\dagger takes on different form other than that of Eq. (94) as we replace $Y_R^\dagger \rightarrow Y_R'^\dagger$. [$Y_R'^\dagger$ are the other forms of K' as catalogued in Eq. (98)].

Referring to M_R in Eq. (28), since we know that, with the ansatz of Eq. (88) and the choice of basis, the matrices $M_l, V, U^\dagger, M_E, Y_L$ are diagonal, it then follows that the form of M_R goes like

$$M_R \sim U^\dagger M_u Y_R^\dagger \sim \begin{pmatrix} \times & 0 & 0 \\ 0 & 0 & \times \\ 0 & \times & 0 \end{pmatrix}. \quad (103)$$

^{†††}Note that the solar neutrino problem can be solved in the current scenario if we mirror symmetrize the model as we did in section VI so that maximal $\nu_e \rightarrow \nu'_e$ oscillations result. In particular if we want to explore the possibility that the atmospheric neutrino anomaly is solved via near maximal $\nu_\mu \rightarrow \nu_\tau$ oscillations then this is actually *compatible* with mirror symmetry, since we just need to be in the parameter region where the oscillation length for $\nu_\mu \rightarrow \nu'_\mu$ oscillations is much greater than the diameter of the earth for atmospheric neutrino energies.

When Y_R^\dagger is replaced by $Y_R'^\dagger$ via some transformation T ,

$$Y_R^\dagger \rightarrow Y_R'^\dagger = TY_R^\dagger, \quad (104)$$

the lop-sided form of M_R should be preserved,

$$U^\dagger M_u Y_R^\dagger \rightarrow U'^\dagger M_u T Y_R^\dagger \sim \begin{pmatrix} \times & 0 & 0 \\ 0 & 0 & \times \\ 0 & \times & 0 \end{pmatrix}. \quad (105)$$

Since $Y_R^\dagger = \begin{pmatrix} 1 & 0 & 0 \\ 0 & 0 & 1 \\ 0 & 1 & 0 \end{pmatrix}$ [see Eq. (94)], this mean that U'^\dagger ought to conform to the condition that

$$U'^\dagger M_u T = \begin{pmatrix} \times & 0 & 0 \\ 0 & \times & 0 \\ 0 & 0 & \times \end{pmatrix}. \quad (106)$$

The matrix T relates the ‘original’ form of Y_R^\dagger [as in Eq. (94)] to $Y_R'^\dagger$ via Eq. (104). Once we know T then we could work out U'^\dagger from Eq. (106). With $Y_R^\dagger \rightarrow Y_R'^\dagger$ and $U^\dagger (= \mathbf{I}) \rightarrow U'^\dagger$, the net effect is that the diagonal up-type quark mass matrix M_u is replaced by

$$M_u \rightarrow U'^\dagger M_u T, \quad (107)$$

thus changing the up-type quark masses dependence of the eigen masses m_i .

(a) $Y_R'^\dagger \equiv K'_4(\delta = 0) = K'_2(\beta = \frac{\pi}{2})$:

Let’s look at the form of $Y_R'^\dagger \equiv K'_4(\delta = 0) = K'_2(\beta = \frac{\pi}{2}) = \begin{pmatrix} 0 & 1 & 0 \\ 0 & 0 & 1 \\ 1 & 0 & 0 \end{pmatrix}$. The corresponding

T matrix is $T = \begin{pmatrix} 0 & 0 & 1 \\ 0 & 1 & 0 \\ 1 & 0 & 0 \end{pmatrix}$. The matrix U'^\dagger , by Eq. (106), is $U'^\dagger = \begin{pmatrix} 0 & 0 & 1 \\ 0 & 1 & 0 \\ 1 & 0 & 0 \end{pmatrix}$,

$$\Rightarrow M_u = \text{diag} \{m_u, m_c, m_t\} \rightarrow U'^\dagger M_u T = \text{diag} \{m_t, m_c, m_u\}. \quad (108)$$

As a result, the up-type quark masses as appear in $m_{2,3}$ and m_1 in Eq. (91) and (102) will be permuted by Eq. (108) which lead to the eigen masses for the light neutrinos

$$m_2, m_3 \approx \mp \eta^2 S^2 M_{E_2} \left(\frac{m_\tau}{m_c} \right), \quad m_1 = -\frac{\eta^2 S^2 M_{E_1}}{2} \left(\frac{m_e}{m_t} \right). \quad (109)$$

We see that the upper limit of the scale of $m_{2,3}^2$ are of the order

$$m_{2,3}^2/\text{eV}^2 \lesssim 200\eta^4, \quad (110)$$

which permits a large range of parameter in η so that $m_{2,3}^2 \gg \delta m_{atm}^2$ for self consistency. The mass gap

$$|m_2^2 - m_1^2| \approx m_2^2 = S^4 \eta^4 M_{E_2}^2 \left(\frac{m_\tau}{m_c} \right)^2 \quad (111)$$

also permits a large range of parameter space in η to accommodate δm_{LSND}^2 . This scheme is easily realised by imposing the ansatz that the Yukawas are of the forms

$$\lambda_2 = \begin{pmatrix} \times & 0 & 0 \\ 0 & \times & 0 \\ 0 & 0 & \times \end{pmatrix}, \quad \lambda_1 = \begin{pmatrix} 0 & 0 & \times \\ 0 & \times & 0 \\ \times & 0 & 0 \end{pmatrix}, \quad \lambda_{3,4} = \begin{pmatrix} 0 & \times & 0 \\ 0 & 0 & \times \\ \times & 0 & 0 \end{pmatrix}. \quad (112)$$

(b) $Y_R^\dagger \equiv K'_1(\alpha = 0) = K'_3(\gamma = \frac{\pi}{2})$:

Next, we look at the form $Y_R^\dagger \equiv K'_1(\alpha = 0) = K'_3(\gamma = \frac{\pi}{2}) = \begin{pmatrix} 0 & 0 & 1 \\ 1 & 0 & 0 \\ 0 & 1 & 0 \end{pmatrix}$. In this case, U^\dagger and T assume the forms

$$U^\dagger = \begin{pmatrix} 0 & 1 & 0 \\ 1 & 0 & 0 \\ 0 & 0 & 1 \end{pmatrix}, \quad T = \begin{pmatrix} 0 & 1 & 0 \\ 1 & 0 & 0 \\ 0 & 0 & 1 \end{pmatrix}. \quad (113)$$

This results in permutation of up-type quark masses $\{m_u, m_c, m_t\} \rightarrow \{m_c, m_u, m_t\}$. The mass square difference

$$|m_2^2 - m_1^2| \approx m_2^2 = S^4 \eta^4 M_{E_3}^2 \left(\frac{m_\mu}{m_t} \right)^2 \lesssim 10^{-7} \left(\frac{M_{E_3}}{\text{TeV}} \right)^2 \text{ eV}^2 \quad (114)$$

is not compatible with the experimental values of δm_{LSND}^2 . In addition, the scale of $m_{2,3}^2$ is also too tiny to accommodate δm_{atm}^2 :

$$m_{2,3}^2 < 4 \times 10^{-5} \text{ eV}^2. \quad (115)$$

In passing, we note that the Yukawas of the forms

$$\lambda_2 = \begin{pmatrix} \times & 0 & 0 \\ 0 & \times & 0 \\ 0 & 0 & \times \end{pmatrix}, \quad \lambda_1 = \begin{pmatrix} 0 & \times & 0 \\ \times & 0 & 0 \\ 0 & 0 & \times \end{pmatrix}, \quad \lambda_{3,4} = \begin{pmatrix} 0 & 0 & \times \\ \times & 0 & 0 \\ 0 & \times & 0 \end{pmatrix} \quad (116)$$

will lead to the above unsatisfactory scheme.

(c) $Y_R^\dagger \equiv K'_1(\alpha = \frac{\pi}{2}) = K'_4(\delta = \frac{\pi}{2})$:

Finally, we investigate the case $Y_R^\dagger \equiv K'_1(\alpha = \frac{\pi}{2}) = K'_4(\delta = \frac{\pi}{2}) = \begin{pmatrix} 0 & 0 & 1 \\ 0 & 1 & 0 \\ 1 & 0 & 0 \end{pmatrix}$. In this case,

U^\dagger and T assume the forms

$$U^\dagger = \begin{pmatrix} 0 & 0 & 1 \\ 1 & 0 & 0 \\ 0 & 1 & 0 \end{pmatrix}, \quad T = \begin{pmatrix} 0 & 1 & 0 \\ 0 & 0 & 1 \\ 1 & 0 & 0 \end{pmatrix}. \quad (117)$$

The up-quark mass permutation is $\{m_u, m_c, m_t\} \rightarrow \{m_t, m_u, m_c\}$. The upper bound of the scale of $m_{2,3}^2$ is

$$m_{2,3}^2/eV^2 \lesssim 0.7\eta^4, \quad (118)$$

which means that it is possible to accommodate δm_{atm}^2 . The mass squared difference for LSND is

$$\delta m_{LSND}^2 \equiv |m_2^2 - m_1^2| \approx m_2^2 = S^4 \eta^4 M_{E_3}^2 \left(\frac{m_\mu}{m_c}\right)^2 \lesssim 10^{-2} \left(\frac{M_{E_3}}{\text{TeV}}\right)^2 eV^2. \quad (119)$$

In this case we see that its parameter space can still accommodate the LSND and atmospheric neutrino anomalies [although the regime of parameter space is more restricted compared to the case (a)]. This scheme can be implemented if the Yukawas take the forms

$$\lambda_2 = \begin{pmatrix} \times & 0 & 0 \\ 0 & \times & 0 \\ 0 & 0 & \times \end{pmatrix}, \quad \lambda_1 = \begin{pmatrix} 0 & 0 & \times \\ 0 & \times & 0 \\ \times & 0 & 0 \end{pmatrix}, \quad \lambda_{3,4} = \begin{pmatrix} 0 & \times & 0 \\ 0 & 0 & \times \\ \times & 0 & 0 \end{pmatrix}. \quad (120)$$

In short, we see that out of the 4 different forms of K' in Eq. (98), the schemes (a) and (c) stand out to be most promising to provide viable solutions to both LSND and (near maximal oscillations) atmospheric neutrino anomaly with mass scale \lesssim few TeV. Note the schemes we have discussed in this section cannot accommodate solar neutrino anomaly (while keeping both LSND and atmospheric neutrino solutions) because the right-handed neutrinos are decoupled from the left-handed ones at TeV scale.

In the parameter range where scalar interactions dominate over the gauge interactions things are less constrained and there are more possibilities. It is possible to implement the lop-sided M_R scheme in the scalar sector case in much the same way as in the previous section. Other possibilities where m_D is off diagonal is also possible in the scalar case which can also lead to schemes compatible with data. However these schemes seem less elegant because of the larger degree of arbitrariness in scalar interactions.

VIII. CONCLUSION

The similarity of the quarks and leptons suggests that quarks and leptons might be connected by some spontaneously broken symmetry. However such a situation will lead to a gauge hierarchy problem unless the symmetry breaking scale is less than a few TeV. There are only two known ways that quark-lepton unification can occur at the TeV scale. First, quarks and leptons can be connected by a spontaneously broken discrete symmetry [2]. While this is an interesting possibility, it is difficult to naturally explain the lightness of the neutrinos in these schemes. The second possibility is a modification of the Pati-Salam model [1] called the alternative 422 model [5,9]. It turns out that the neutrinos in the alternative 422 model are naturally light because they are massless at the tree level and their masses are radiatively generated. The model also predicts novel B^o physics.

The possibility that the model can provide the interactions to generate the right neutrino mass and mixing patterns which might explain the atmospheric, solar and/or LSND neutrino

anomalies has been studied in detail in this paper. We have shown that the model cannot accommodate simultaneously all three of the anomalies unless it is extended in some way. However the minimal model can quite naturally accommodate the atmospheric and LSND anomalies. We have also pointed out that the solar neutrino problem could be most naturally explained if the model was extended with a mirror sector.

Acknowledgements

R.Foot is an Australian Research Fellow.

T.L.Yoon is supported by OPRS and MRS from The University of Melbourne.

Appendix

In this Appendix we will obtain the precise form of the would-be Goldstone bosons $G_{L,R}^\pm$ and physical Higgs fields $H_{1,2}^\pm$ in terms of the charged weak eigenstate fields $\chi_{L,R}^{4,-\frac{1}{2}}$, $\phi^{\frac{1}{2},\frac{1}{2}}$ and $\phi^{-\frac{1}{2},-\frac{1}{2}}$ [i. e. the matrix U_g in the Eq. (43)]. In addition we will also obtain the interesting result that

$$\lim_{\substack{u_1 \rightarrow 0 \\ u_2 \neq 0}} V_{3\langle\phi\rangle} = \lim_{\substack{u_2 \rightarrow 0 \\ u_1 \neq 0}} V_{3\langle\phi\rangle} = 0. \quad (121)$$

The Goldstone bosons associated with each spontaneously broken symmetry are given by

$$G = \Phi^T T^a \lambda_a, \quad (122)$$

where Φ are the Higgs scalar of the theory, T^a the generators of the broken symmetries and λ_a the vacua. G_L^\pm is the would-be Goldstone bosons that are eaten by W_L^\pm as their longitudinal polarisation. The associated (charged) generators of the broken $SU(2)_L$ are τ_L^\pm . Generally,

$$G_L^\pm = \left[\chi_L^T \tau_L^\pm \langle \chi_L \rangle + \chi_L^{cT} \tau_L^\pm \langle \chi_L^c \rangle + \chi_R^T \tau_L^\pm \langle \chi_R \rangle + \chi_R^{cT} \tau_L^\pm \langle \chi_R^c \rangle + \phi^T \tau_L^\pm \langle \phi \rangle + (\phi^c)^T \tau_L^\pm \langle \phi^c \rangle \right] \frac{1}{N_L}. \quad (123)$$

For definiteness let us focus on the negatively charged fields, and let us work in the limit $u_1 \rightarrow 0$:

$$G_L^- = \frac{1}{\sqrt{u_2^2 + w_L^2}} \left[w_L \chi_L^{4,-\frac{1}{2}} + u_2 \phi^{-\frac{1}{2},-\frac{1}{2}} \right]. \quad (124)$$

Likewise, G_R^\pm are associated with the SSB of charged sector in $SU(2)_R$:

$$G_R^\pm = \left[\chi_L^T \tau_R^\pm \langle \chi_L \rangle + \chi_L^{cT} \tau_R^\pm \langle \chi_L^c \rangle + \chi_R^T \tau_R^\pm \langle \chi_R \rangle + \chi_R^{cT} \tau_R^\pm \langle \chi_R^c \rangle + \phi^T \tau_R^\pm \langle \phi \rangle + (\phi^c)^T \tau_R^\pm \langle \phi^c \rangle \right] \frac{1}{N_R}, \quad (125)$$

from which we obtain

$$G_R^- = -\frac{1}{\sqrt{u_2^2 + w_R^2}} \left[w_R \chi_R^{4,-\frac{1}{2}} - u_2 (\phi^{\frac{1}{2},\frac{1}{2}})^* \right]. \quad (126)$$

The states orthogonal to $G_{L,R}^\pm$ will be the physical Higgs $H_{1,2}^\pm$ which in general not uniquely fixed because there are 2 directions orthogonal to $G_{L,R}^\pm$.

A particularly important term in the Higgs potential is the term responsible for mixing $\chi_L^{4,-\frac{1}{2}}$ with $\chi_R^{4,-\frac{1}{2}}$ which effects the generation of Dirac masses of neutrinos in the χ -loop,

$$V_3 = M\chi_L^\dagger\phi\tau_2\chi_R + M'\chi_L^\dagger\phi^c\tau_2\chi_R + \text{H.c.} \quad (127)$$

We will show that there exists an approximate global symmetry $U(1)_X$ of this Higgs potential in the limit $u_1 \rightarrow 0, u_2 \neq 0$ (or $u_2 \rightarrow 0, u_1 \neq 0$) that will allow us to identify the physical Higgs states (in that limit). The global symmetry $U(1)_X$ can be defined by the generator

$$X = Y' + I_{3R} - I_{3L}, \quad (128)$$

where

$$Y'\langle\chi_R\rangle = -\frac{1}{2}, \quad Y'\langle\chi_L\rangle = \frac{1}{2}, \quad Y'\langle\phi\rangle = 1. \quad (129)$$

Furthermore for the global symmetry to be useful we require it to be unbroken by the vacuum, that is,

$$X\langle\chi_L\rangle = X\langle\chi_R\rangle = X\langle\phi\rangle = 0 \quad (130)$$

which is indeed the case given our choice of X (and the limit $u_1 \rightarrow 0$).

Referring to V_3 in Eq. (127), notice that the M' term is not a symmetry under $U(1)_X$. However, in the limit $u_1 \rightarrow 0$ then M' must also be zero for self consistency. The reason is that a non zero M' in V_3 will induce a linear term in the (21) component of ϕ (i.e. the place where u_1 would sit) when $\chi_{L,R}$ develop VEVs. Because the potential is linear in u_1 (for small u_1) a non-zero VEV for u_1 must arise which is obviously not self consistent with our assumption that $u_1 = 0$. This shows that $U(1)_X$ becomes an unbroken symmetry because the $U(1)_X$ asymmetry M' term vanishes in the limit $u_1 \rightarrow 0$. (We can also draw similar conclusion in the limit $u_2 \rightarrow 0, u_1 \neq 0$.) Furthermore it allows us to uniquely specify the physical Higgs fields H_1, H_2 since now we have two requirements. First they must be orthogonal to $G_{L,R}$ and second they must be composed of components with the same $U(1)_X$ charge. (Note that H_1 has X -charge -1, H_2 has X -charge +1.) These considerations lead to the identification of the charged physical Higgs fields:

$$\begin{aligned} H_1^- &= \frac{1}{u_2\sqrt{1+(u_2/w_R)^2}} \left[\frac{u_2^2}{w_R} \chi_R^{4,-\frac{1}{2}} + u_2(\phi^{\frac{1}{2},\frac{1}{2}})^* \right], \\ H_2^- &= -\frac{1}{u_2\sqrt{1+(u_2/w_L)^2}} \left[\frac{u_2^2}{w_L} \chi_L^{4,-\frac{1}{2}} - u_2\phi^{-\frac{1}{2},-\frac{1}{2}} \right]. \end{aligned} \quad (131)$$

Writing Eq. (124), (126), (131) in matrix form, we obtain Eq. (43). Note that the matrix U_g is unitary, $U_g^{-1} = U_g^T$ because the rows (and columns) are all orthogonal. The existence of the approximate global symmetry X in the limit $u_1 \rightarrow 0, u_2 \neq 0$ (or $u_2 \rightarrow 0, u_1 \neq 0$) means that the mass mixing term

$$V_{3\langle\phi\rangle} \propto u_1 u_2. \quad (132)$$

The effect of this is that we can treat the mass mixing terms $V_{3\langle\phi\rangle} = -(Mu_1 + M'u_2)\chi_L^{4,-\frac{1}{2}}\chi_R^{4,-\frac{1}{2}*}$ as a small perturbation when u_1 (u_2) is switched on from zero.

REFERENCES

- [1] J. Pati and A. Salam, Phys. Rev. D 10 (1974) 275.
- [2] R. Foot and H. Lew, Phys. Rev. D 41 (1990) 3502; Nuovo Cimento A104, 167 (1991); R. Foot, H. Lew and R.R. Volkas, Phys. Rev. D 44 (1991) 1531.
- [3] G. Valencia and S. Willenbrock, Phys. Rev. D50, 6843 (1994); A. V. Kuznetsov and N. V. Mikheev, Phys. Lett. B 329, 295 (1994); R. R. Volkas, Phys. Rev. D53, 2681 (1996); A. D. Smirnov, Phys. Lett. B431, 119 (1998).
- [4] H. Harari and Y. Nir, Nucl. Phys. B292, 251 (1987).
- [5] R. Foot, Phys. Lett. B 420 (1998) 333.
- [6] T. Haines et al., Phys. Rev. Lett. 57 (1986) 1986; Kamiokande Collaboration, K.S. Hirata et al., Phys. Lett. B 205 (1998) 416; *ibid.* B 280 (1992) 146; *ibid.* B 335 (1994) 237; IMB Collaboration, D. Casper et al., Phys. Rev. Lett. 66 (1989) 2561; R. Becker-Szendy et al., Phys. Rev. D 46 (1989) 3720; Nussex Collaboration, M. Aglietta et al., Europhys. Lett. 8 (1989) 611; Frejus Collaboration, Ch. Berger et al., Phys. Lett. B 227 (1989) 489; *ibid.* B 245 (1990) 305; K. Daum et al, Z. Phys. C 66 (1995) 417; Soudan 2 Collaboration, W.W.M., Allison et. al., Phys. Lett. B 391 (1997) 491; SuperKamiokade Collaboration, Y. Fukuda et al., Phys. Lett. B 433 (1998) 9; Phys. Lett. B 436 (1998) 33; Phys. Rev. Lett. 81 (1998) 1562; MACRO Collaboration, M. Ambrosio et al, Phys. Lett. B 434 (1998) 451.
- [7] Homestake Collaboration, B. T. Cleveland et al., Astrophys. J. 496 (1998) 505; Kamiokande Collaboration, Y. Fukuda et al., Phys. Rev. Lett. 77 (1996) 1683; S. Fukuda, hep-ph/0103032; SAGE Collaboration, J. N. Abdurashitov et al., Phys. Rev. Lett. 83 (1999) 4686; GALLEX Collaboration, W. Hampel et al., Phys. Lett. B 447 (1999) 127; GNO Collaboration, M. Altmann et al., Phys. Lett. B490, 16 (2000).
- [8] LSND Collaboration, W. Athanassopoulos et al., Phys. Rev. Lett. 81 (1998) 1774; Phys. Rev. C 58 (1998) 2489.
- [9] R. Foot and G. Filewood, Phys. Rev. D 60 (1999) 115002.
- [10] R. Foot, R.R. Volkas, O. Yasuda, Phys. Rev. D 58 (1998) 013006; P. Lipari, M. Lusignoli, Phys. Rev. D 58 (1998) 073005.
- [11] S. Fukuda et al., Phys. Rev. Lett. 85 (2000) 3999.
- [12] R. Foot, Phys. Lett. B 496 (2000) 169.
- [13] G. Conforto et al, Astropart. Phys. 5 (1996) 147 ; Phys. Lett. B 427 (1998) 314.
- [14] A. H. Guth, L. Randall and M. Serna, JHEP 9908 (1999) 018 .
- [15] R. Foot and R. R. Volkas, hep-ph/9510312 and also Ref. [34].
- [16] R. Foot, Phys. Lett. B 483 (2000) 151.
- [17] R. Crocker, R. Foot and R. R. Volkas, Phys. Lett. B 465 (1999) 203.
- [18] R. Foot and R. R. Volkas, Phys. Rev. D 55 (1997) 5147.
- [19] CHOOZ Collaboration, M. Apollonio et al., Phys. Lett. B 420 (1998) 397; Palo Verde Collaboration, F. Boehm et al, Phys. Rev. Lett. 84 (2000) 3764; Phys. Rev. D 62 (2000) 072002.
- [20] Super-Kamiokande Collaboration, S. Fukuda, hep-ex/0103032.
- [21] Super-Kamiokande Collaboration, S. Fukuda, hep-ex/0103033.
- [22] SNO Collaboration, nucl-ex/0106015.
- [23] see the Borexino website, <http://almime.mi.infn.it/>.

- [24] see the KamLAND website, <http://www.awa.tohoku.ac.jp/html/KamLAND/>.
- [25] J. Bunn, R. Foot and R. R. Volkas, Phys. Lett. B 413 (1997) 109; R. Foot, R. R. Volkas and O. Yasuda, Phys. Rev. D (1998) 1345.
- [26] <http://www.neutrino.lanl.gov/BooNE/>.
- [27] G. Raffelt and D. Seckel, Phys. Rev. Lett. 60 (1988) 1793.
- [28] R. Barbieri and R. N. Mohapatra, Phys. Rev. D 39 (1989) 1229.
- [29] P. Langacker and S. U. Sankar, Phys. Rev. D 40 (1989) 1569.
- [30] V. Berezhinsky, in *The Ninth International Workshop on Neutrino Telescopes*, Venice, astro-ph/0107306 (2001).
- [31] M. S. Tuner, Phys. Rev. Lett. 60 (1988) 1797.
- [32] K. Kanaya, Prog. Theor. Phys. 64 (1980) 2287.
- [33] T. L. Yoon and R. Foot, Phys. Lett. B 491 (2000) 291; B. C. Allanach, Phys. Lett. B 450 (1999) 182.
- [34] R. Foot, H. Lew and R. R. Volkas, Phys. Lett. B 272 (1991) 67; R. Foot, H. Lew and R. R. Volkas, Mod. Phys. Lett. A 7 (1992) 2567; R. Foot, Mod. Phys. Lett. A 9 (1994) 169; R. Foot, R. R. Volkas, Phys. Rev. D 52 (1995) 6595.
- [35] R. Foot, astro-ph/0102294.